Research Paper

THEMED ISSUE: Exploring the Deep Sea and Beyond, Volume 2

GEOSPHERE

GEOSPHERE; v. 12, no. 1

doi:10.1130/GES01233.1

15 figures; 1 table

CORRESPONDENCE: e.pemberton@ucalgary.ca

CITATION: Pemberton, E.A.L., Hubbard, S.M., Fildani, A., Romans, B., and Stright, L., 2016, The stratigraphic expression of decreasing confinement along a deep-water sediment routing system: Outcrop example from southern Chile: Geosphere, v. 12, no. 1, doi:10.1130/GES01233.1.

Received 16 July 2015
Revision received 11 November 2015
Accepted 23 December 2015

The stratigraphic expression of decreasing confinement along a deep-water sediment routing system: Outcrop example from southern Chile

Erin A.L. Pemberton[1,*], Stephen M. Hubbard[1], Andrea Fildani[2,†], Brian Romans[3], and Lisa Stright[4]

[1]Department of Geoscience, University of Calgary, 2500 University Drive NW, Calgary, Alberta T2N 1N4, Canada
[2]Chevron Energy Technology Company, 6001 Bollinger Canyon Road, San Ramon, California 94583, USA
[3]Department of Geosciences, Virginia Tech, 4044 Derring Hall (0420), Blacksburg, Virginia 24061, USA
[4]Department of Geosciences, Colorado State University, 322 Natural Resources Building, Fort Collins, Colorado 80523, USA

ABSTRACT

The products of sediment-laden turbidity currents that traverse areas of decreasing confinement on submarine slopes include erosional and depositional features that record the inception and propagation of deep-sea channels. The cumulative stratigraphic expression and deposits of such transitions, however, are poorly constrained relative to depositional settings dominated by end-member confined (i.e., submarine channel fill) and unconfined (i.e., lobe) deposits. Upper Cretaceous strata of the Magallanes foreland basin in southern Chile are characterized by a variety of stratigraphic architectural elements in close juxtaposition both laterally and vertically, including: (1) low-aspect-ratio channelform bodies attributed to slope channel fills; (2) high-aspect-ratio channelform bodies interpreted as the deposits of weakly confined submarine channels; (3) lenticular sedimentary bodies considered to represent the infill of laterally coalesced scours; (4) discontinuous channelform bodies representing isolated scour fills; and (5) a cross-stratified, positive-relief sedimentary body, which is interpreted to record an upslope-migrating depositional bedform. These elements are interpreted to have formed at a submarine sediment routing system segment characterized by a break in slope, and an accompanying decrease in confinement. The various architectural elements examined are interpreted to record a unique stratigraphic perspective of turbidite channels at various stages of development, from early-stage discontinuous and isolated scour fills to low-aspect-ratio channel units.

INTRODUCTION

Sandstone-prone sedimentary bodies and component beds from deep-water strata contain critical information about the processes of sediment transfer in poorly constrained slope settings (e.g., Mutti and Normark, 1987, 1991; Hubbard et al., 2014) and the distribution of reservoirs within petroliferous continental margins around the globe (e.g., Posamentier and Kolla, 2003; Mayall et al., 2006; Deptuck et al., 2003, 2007). Two end-member sedimentary body architectural styles are most commonly considered: channelform fill and lobate or sheet like (Fig. 1). They are expressed at a range of scales, and observed in many different types of data including seismic reflection (e.g., Gulf of Mexico, Posamentier, 2003; offshore Nigeria, Deptuck et al., 2003), modern seafloor and/or shallow subsurface (e.g., Lucia Chica channel system, Maier et al., 2011, 2013; La Jolla fan, Normark, 1970; Navy fan, Normark et al., 1979), and outcrop (e.g., Brushy Canyon Formation, Beaubouef et al., 1999, Gardner et al., 2003; Karoo Basin, Prélat et al., 2010, Hodgson et al., 2011). However, the stratigraphic expression of transitional segments of a sediment-routing system, spatially between confined channels, weakly confined channels, and

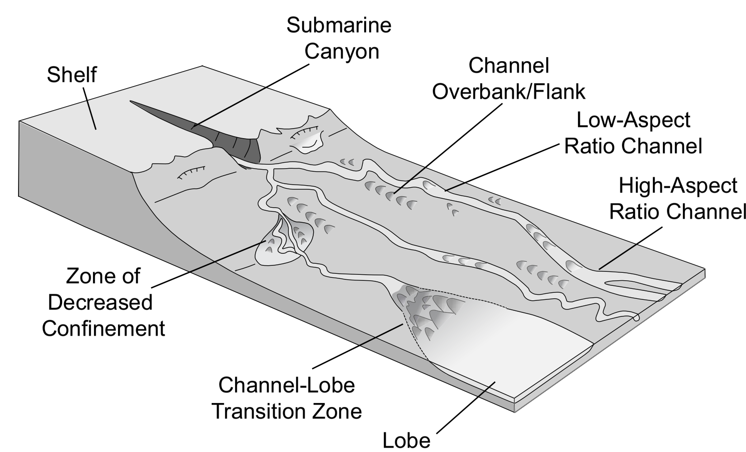

Figure 1. Schematic diagram of deep-water sediment-routing systems. The locations discussed herein include intraslope zones of decreasing confinement, channel-lobe transition zones, overbank and/or channel flank, and intrachannel areas.

*Present address: ConocoPhillips, Global New Ventures Exploration, 600 N. Dairy Ashford, Houston, Texas 77079, USA.
†Present address: Statoil RDI, Research Center Austin, Austin, Texas 78730, USA.

unconfined lobes, remains elusive or not as well documented in these same data sets (Fig. 1). Discrimination of channel-lobe transition zone deposits in outcrops has been a recent emphasis (e.g., Morris et al., 2014; Van der Merwe et al., 2014; Marini et al., 2015), although transitions from confined to weakly confined channels have not been emphasized despite their prevalence in seafloor and seismic data sets (e.g., Adeogba et al., 2005; Gee and Gawthorpe, 2007; McHargue et al., 2011; Maier et al., 2012). It is plausible that recognition of these deposits in the outcrop sedimentary record has been hindered by lack of a clear set of defining criteria.

In this study, slope deposit outcrops (Upper Cretaceous Tres Pasos Formation, Magallanes Basin) are studied in order to determine the stratigraphic expression of turbidity currents transitioning from confined to less confined segments of a deep-water sediment-routing system. Depositional context is critical for interpreting the nature of these potential flow transitions in the rock record (e.g., Mutti and Normark, 1987, 1991; Vicente Bravo and Robles, 1995; Elliott, 2000; Fildani and Normark, 2004; Fildani et al., 2013), and the established slope position for the Tres Pasos Formation outcrop of interest provides the necessary foundation for this analysis (Fig. 2; Hubbard et al., 2010).

Our interpretation of this outcrop is necessarily guided and instructed by observations from the modern seafloor (e.g., Normark et al., 1979; Normark and Piper, 1983; Wynn et al., 2002; Maier et al., 2011, 2013) and by experimental (Rowland et al., 2010) and numerical insights (Kostic, 2014). Recently resolved seafloor geomorphologies, including large-scale scours or flute-shaped depressions, have been documented in diverse deep-water environments and interpreted as the expression of rapid flow transition; settings include proximal levee and overbank settings, the bases of deep-sea channels, intraslope zones characterized by changes in seafloor slope, and channel-lobe transition zones (Fig. 1; Shor et al., 1990; Wynn et al., 2002; Kostic and Parker, 2006; Kostic, 2011; Maier et al., 2011; Cartigny et al., 2011; Macdonald et al., 2011).

Theoretically, as turbidity flows pass from confined to less confined segments of a sediment-routing system, they expand and thicken; this has a profound impact on flow properties (Garcia and Parker, 1989). This transition is therefore commonly interpreted to influence erosion and deposition and, after a protracted period of sediment transfer, the resulting stratigraphic architecture. Changes in flow characteristics are common in different settings, including zones where flows encounter an abrupt decrease in slope such as intraslope minibasins (e.g., Prather et al., 1998; Pirmez et al., 2000; Prather, 2003), and areas where flows pass through breaches in channel banks and spread into an overbank setting (e.g., Flood et al., 1995; Posamentier and Kolla, 2003; Fildani et al., 2006; Jegou et al., 2008). The manifestations of these zones in the rock record, although only sporadically described, are characterized by a spectrum of bed-scale features (e.g., Cazzola et al., 1981; Mutti and Normark, 1987, 1991), as well as juxtaposition of various architectural elements, including (1) low-aspect-ratio (i.e., width:thickness) channelform units, and (2) broad, high-aspect-ratio to tabular sedimentary bodies (i.e., channelform to more lobate; Cazzola et al., 1981; Mutti and Normark, 1987, 1991).

The primary objective of this work is to establish sedimentological and architectural criteria for recognition of flow transition deposits in the ancient record, specifically those associated with decreasing confinement of submarine channels downslope. We present evidence for the stratigraphic products of submarine channels at various stages of development, from incipient scour to terminal infilling.

PALEOGEOGRAPHIC SETTING AND BASIN STRATIGRAPHY

The Magallanes retroarc foreland basin of southern Chile parallels the Andean fold-thrust belt (Fig. 2; Fildani and Hessler, 2005; Romans et al., 2010; Fosdick et al., 2011). The basin consists of 4–5 km of Upper Cretaceous deep-water strata, including unconfined deposits of the Punta Barrosa Formation, overlying deep-marine channel belt deposits of the Cerro Toro Formation, and a progradational slope system consisting of genetically related slope deposits of the Tres Pasos Formation and deltaic units of the Dorotea Formation (Fig. 3; Romans et al., 2011). The 1.5–2-km-thick Tres Pasos and Dorotea Formations record southward axial infill of the foredeep by slope clinoforms that were 400–1000 m thick (Fig. 3; Hubbard et al., 2010; Bauer, 2012). The ~100-m-thick stratigraphic interval of interest to this study is located ~40 km southward from coeval shelf-edge deposits, and deposition is considered to have taken place toward the lower portion of a high-relief (>900 m) slope (Fig. 3; cf. Hubbard et al., 2010). The strata transition up the paleoslope to stacked slope channel deposit–dominated units (Fig. 3). These updip units consist of at least 5 distinct slope channel fills, 15–20 m thick and 200–300 m wide each, that stack with varying degrees of lateral and vertical offset. The presence of these updip channel units provides important context regarding upslope to downslope architectural changes in the stratigraphic interval of interest. The stratigraphic interval plunges into the subsurface south of the study area, limiting interpretations about the downslope segment of the ancient sediment routing system.

The Magallanes Basin was characterized by generally high sediment flux recorded by the prograding slope clinoform system (Hubbard et al., 2010; Romans et al., 2010). Elevated aggradation on the paleoslope is hypothesized to have led to regular rapid burial of the studied sediment-routing system segments, which promoted preservation of what are otherwise commonly poorly preserved features such as scour fills; therefore, the outcrop offers a unique opportunity to study commonly elusive formative features in the sedimentary record.

STUDY AREA AND DATA SET

The Tres Pasos Formation outcrop studied is 1500 m long and ~100 m thick, situated adjacent to the Parque Nacional Torres del Paine Highway, ~20 km south of the Villa Cerro Castillo in southern Chile (Fig. 2A). The outcrop comprises strike-oriented and dip-oriented faces; this provides some three-dimensional (3-D) control on sedimentary body geometries (Figs. 2B, 2C).

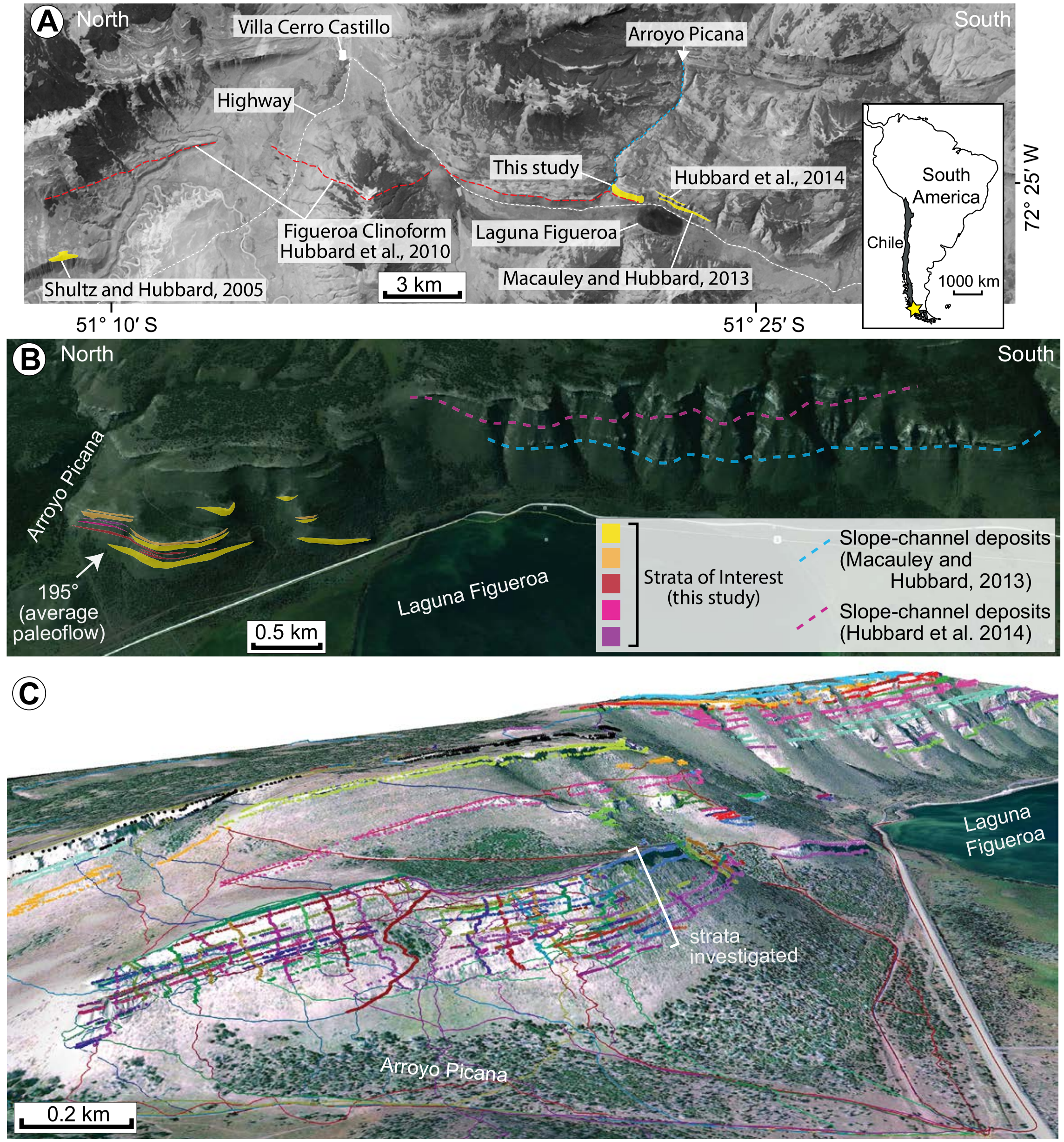

Figure 2. Overview of the area of interest. (A) Satellite image of the Magallanes Basin outcrop belt featuring major landmarks and past studies done in the region (modified from Hubbard et al., 2010); in inset line drawing of South America, yellow star indicates study area. (B) Perspective Google Earth satellite image of the study area featuring Laguna Figueroa at the bottom and the Parque Nacional Torres del Paine Highway adjacent to the outcrop belt. The deposits of interest at Arroyo Picana are highlighted. (C) Southward view of the outcrop of interest; differential global positioning system was used to survey measured section locations and the stratigraphic surfaces that define sedimentary bodies.

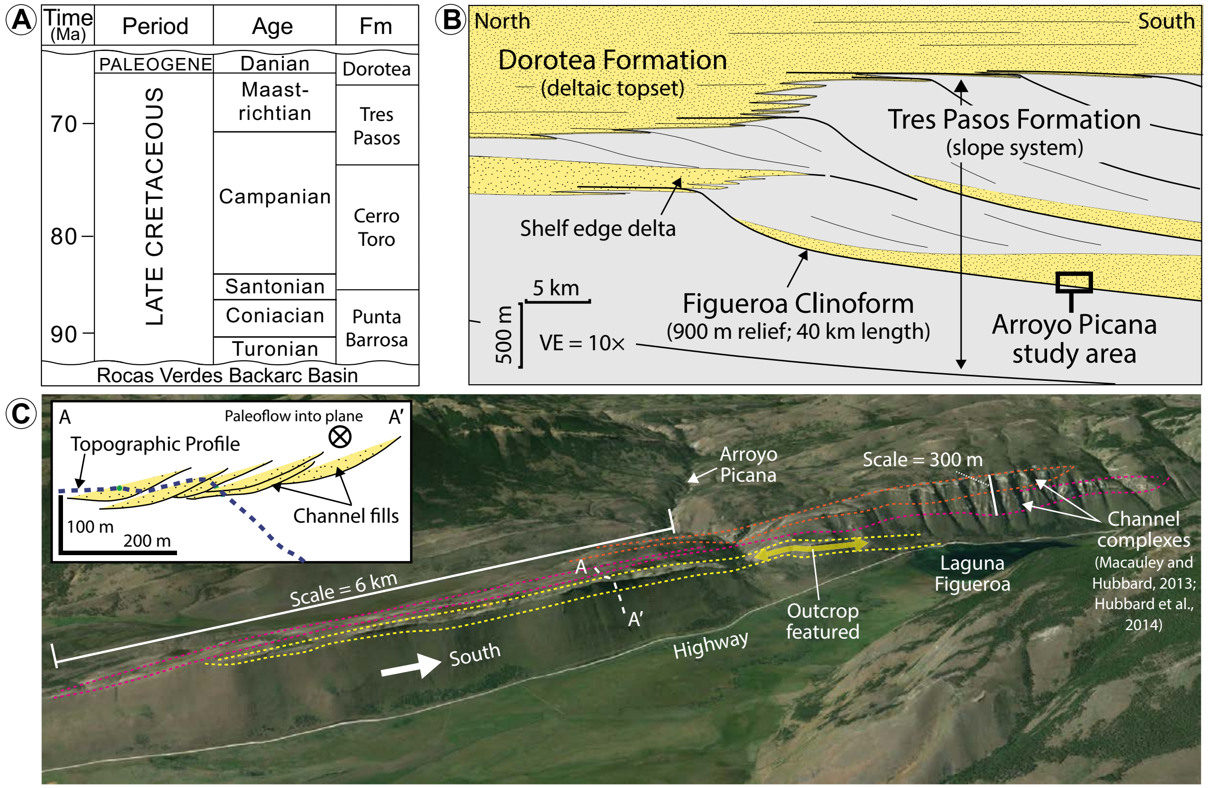

Figure 3. (A) Stratigraphic column of the Magallanes foreland basin. The Punta Barrosa and Cerro Toro Formations (Fm) record deep-water deposition, while the genetically linked Tres Pasos (slope) and Dorotea (deltaic) Formations are associated with the final infill of the deep-water seaway (modified from Hubbard and Shultz, 2008). (B) Tres Pasos–Dorotea slope system overview, showing southward (basin axial) progradation of large (>900 m relief and 40 km long) clinoforms. This study focuses on lower slope deposits of the Tres Pasos Formation (modified from Bauer, 2012). VE—vertical exaggeration. (C) Perspective satellite image from Google Earth showing the outcrop studied at Arroyo Picana, updip stacked channel deposits (inset cross section modified from Daniels, 2015), and overlying channel complexes adjacent to Laguna Figueroa. Strata downdip of the units studied plunge into the subsurface to the south.

The data set consists of 42 stratigraphic sections measured at 10–25 m lateral spacing, for a total of 1624 m of section. Emphasis was placed on bed thickness, nature of bed contacts (e.g., sharp, undulatory), grain-size distribution, and sedimentary structures. Stratigraphic correlation of the closely spaced sections, high-resolution photomosaic interpretation, and surveying beds in the field constrained subtle architectural changes, even among thin and lenticular units. Bed-set boundaries and section locations were surveyed with a differentially corrected, high-resolution (~10 cm) global positioning system (Trimble ProXRT), and the entire data set was used to construct a digital elevation model of the outcrop belt (Fig. 2C). Paleoflow measurements (n = 144) were made at 39 locations, primarily derived from sole marks and ripple cross-lamination.

Surveyed stratigraphic surfaces, facies trends (e.g., thickest and most amalgamated sandstone in flow axes), and paleoflow data were used to map and extrapolate the 3-D trends of architectural elements. Width:thickness, or aspect ratios, are tabulated for strike-oriented cross sections of distinct sedimentary bodies. All data were imported into 3-D modeling software (i.e., Petrel 2013 E&P Software Platform; https://www.software.slb.com/products/petrel), which facilitated visualization and promoted more accurate mapping (Fig. 2C). In order to construct geologically reasonable geometries of sedimentary bodies beyond the outcrop in instances where 3-D exposure was limited, insight was drawn from published examples of other outcrop and high-resolution seafloor analogs.

RESULTS

Sedimentary Facies Associations

Four facies associations are identified and interpreted in the study area (Table 1; Fig. 4). Derived from measured sections, these facies associations represent a key portion of the data set, summarized in Table 1 with accompanying process-based interpretations. In general, the deposits investigated are largely the product of both high- and low-density turbidity currents, as well as a degree of mass transport (cf. Bouma, 1962; Lowe, 1982; Talling et al., 2012; Postma et al., 2014).

TABLE 1. FACIES ASSOCIATIONS OF THE ARROYO PICANA OUTCROP

Facies association (FA)	Lithology, grain size	Sand (%)	FA thickness (m)	Bed thickness	Physical structures	Basal contacts	Lithologic accessories	Process-based interpretation	Lateral relationship to other FAs
FA1: Amalgamated, thick-bedded sandstone	Medium- to fine-grained sandstone	90–100	Variable 0.5–27	Lenticular 0.2–2.5 m	Normal grading, structureless, rare planar and ripple lamination; local dewatering structures	Sharp; planar or slightly undulatory	Angular to subrounded siltstone clasts	High-density turbidity flow; abundant scour (Lowe, 1982; Postma and Cartigny, 2014)	Grades laterally to FA2; flow axis deposits (Mutti and Normark, 1987; McHargue et al., 2011)
FA2: Nonamalgamated, thick-bedded sandstone	Medium- to fine-grained sandstone and siltstone	60–90	Variable 0.1–1	Lenticular 0.1–0.9 m	Structureless, planar and ripple lamination; rare cross-stratification; back-set stratification	Sharp; planar or occasionally undulatory	Angular to subrounded siltstone clasts	High- to low-density turbidity flow (Bouma, 1962; Lowe, 1982); Cyclic steps (Postma and Cartigny, 2014)	Transitions laterally to FA1 and FA3; flow off axis to margin deposits (Hubbard et al., 2014)
FA3: Thinly interbedded siltstone and sandstone	Fine- to very fine-grained sandstone and siltstone	20–50	Variable 0.1–9	Sandstone, <10 cm Siltstone, 5–90 cm	Sandstone: normal grading, planar and ripple lamination Siltstone: planar lamination	Sharp	Abundant organic detritus	Dilute turbidity flows and suspension setting (Bouma, 1962)	In some cases, transitions laterally to FA2; flow margin deposits, also background facies (Hubbard et al., 2014)
FA4: Chaotically bedded siltstone and sandstone	Medium- to very fine-grained sandstone and siltstone	30–70	Variable 0.1–2		Chaotic and/or deformed lamination; dewatering structures	Sharp	Abundant organic detritus	Cohesive debris flow	

Architectural Components

The 2-D to 3-D exposed architectural elements of the Arroyo Picana outcrop belt include (1) low-aspect-ratio (i.e., width:thickness) channelform bodies; (2) high-aspect-ratio channelform bodies; (3) relatively high-aspect-ratio, variably thick and laterally continuous lenticular bodies; (4) discontinuous, low-relief and low-aspect-ratio channelform bodies; and (5) positive relief and discontinuous cross-stratified sandstone units. These architectural components are described in the context of four broadly correlatable sedimentary packages, including unit A at the base up through unit D at the top (Figs. 5 and 6).

Low-Aspect-Ratio Channelform Architecture

Description. Channelform sedimentary bodies 7–20 m thick and 170–375 m wide have aspect ratios between 10 and 20 (Fig. 6). Paleocurrent observations average ~180° and range from 160° to 220° (Fig. 5). Amalgamated sandstone (FA1) is prevalent in the axes of these bodies, transitioning to nonamalgamated thick-bedded sandstone (FA2) and thinly interbedded sandstone and siltstone (FA3) laterally, toward the edges of the channelforms (Fig. 7). Basal surfaces of the bodies truncate underlying strata, and in most instances, are overlain by fine-grained deposits of FA3. This architecture is observed in units A and C (Figs. 5 and 7).

Interpretation. Low-aspect-ratio channelform sedimentary bodies are attributed to processes of erosion, sediment bypass, and ultimately filling of slope channels (cf. Figueiredo et al., 2013; Hubbard et al., 2014). The axis to margin facies transition records relatively high energy in channel thalwegs and lower energy toward the margins (e.g., Mutti and Normark, 1987; Clark and Pickering, 1996; Macauley and Hubbard, 2013). Fine-grained facies directly overlying basal incision surfaces have been attributed to deposition from the tails of high-energy flows that bypassed their coarse-grained load basinward (cf. Mutti and Normark, 1987; Barton et al., 2010; Stevenson et al., 2015). The particularly wide sedimentary body in unit A is considered a composite feature consisting of multiple, partially preserved, laterally stacked channel fills (Fig. 5; cf. channel complex of Campion et al., 2005; Di Celma et al., 2011; McHargue et al., 2011; Stright et al., 2014).

High-Aspect-Ratio Channelform Architecture

Description. High-aspect-ratio channelform sedimentary bodies are 5–10 m thick and 200–500 m wide with aspect ratios between 50 and 60. Paleocurrent observations average ~180° and range from 160° to 200° (Fig. 6). As with the low-aspect-ratio channelform bodies, this architecture is best reflected in the distribution of sandstone-dominated strata (Figs. 5 and 7). Amalgamated sandstone (FA1) is present in the axes of these bodies with fairly abrupt transitions laterally to nonamalgamated thick-bedded sandstone (FA2) and thinly interbedded sandstone and siltstone (FA3) at channelform edges. The basal surface of these channelform bodies is associated with truncation of underlying units, and the architecture is observed in units C (upper) and D (Figs. 6 and 7).

Interpretation. These sedimentary bodies are attributed to processes of erosion, sediment bypass, and infilling of slope channels (cf. Hubbard et al.,

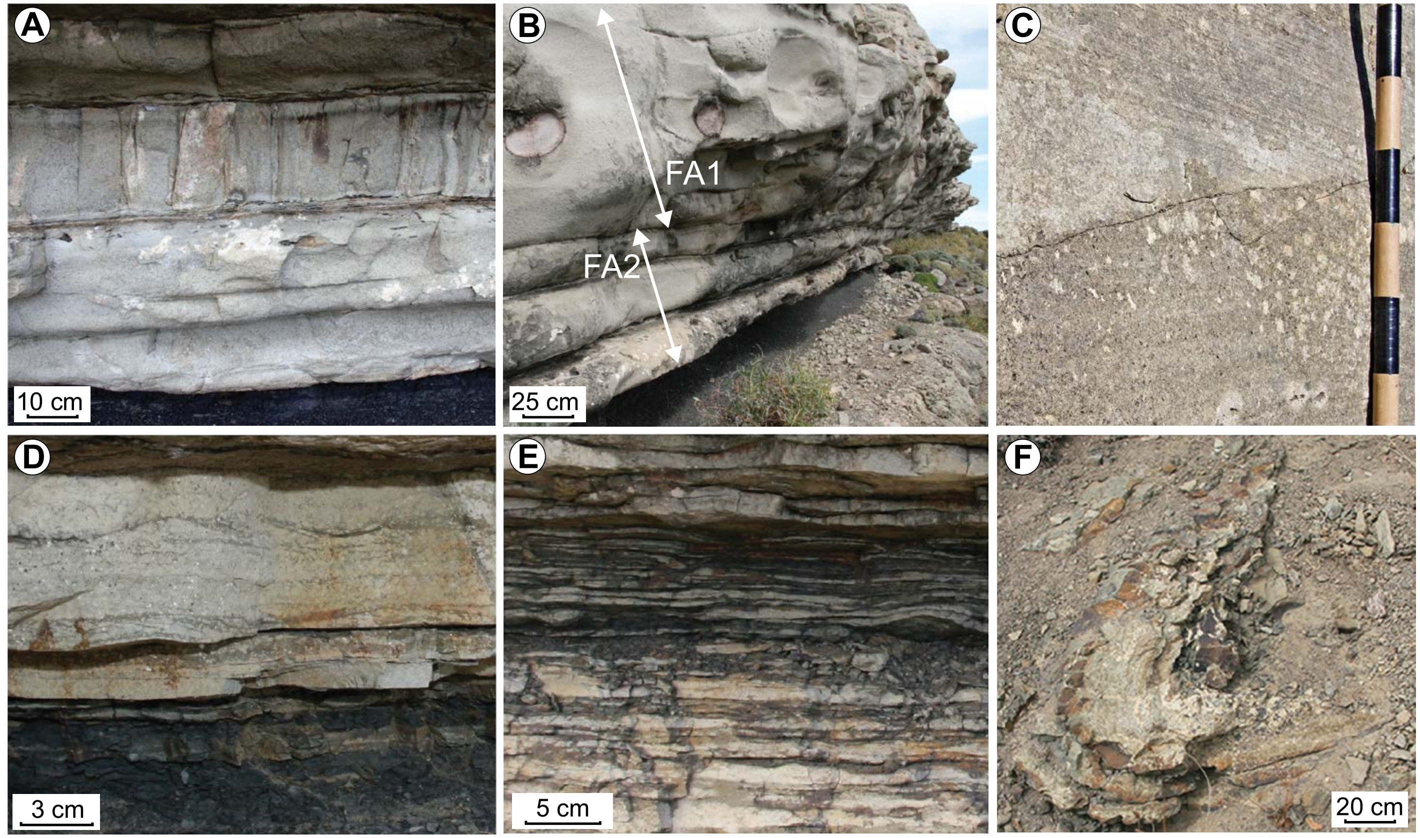

Figure 4. Facies of the Tres Pasos Formation. (A, B) Normally graded structureless to planar laminated (Bouma Ta, Tb) amalgamated sandstone of FA1, with local rip-up clasts. Nonamalgamated thickly bedded sandstone is also present in B (FA2). (C) Cross-stratified sandstone of FA2. Scale indicated by 10 cm demarcations on jake-staff. (D) Thinly interbedded sandstone and siltstone of FA3 overlain by FA2. (E) Interbedded siltstone and sandstone of FA3. (F) Contorted bedding characteristic of FA4.

2014). The shallow and broad channel fills are interpreted as weakly confined turbidite channel elements, which are often found in areas of low to moderate gradient on a paleodepositional profile (Funk et al., 2012; Brunt et al., 2013; Fildani et al., 2013). High-aspect-ratio channels often do not effectively contain thick turbidity currents, and are therefore commonly associated with avulsion (e.g., Maier et al., 2013; Stevenson et al., 2013).

Lenticular Sedimentary Body Architecture

Description. Lenticular sedimentary bodies are 0.8–12 m thick and 37–1150 m wide (aspect ratios 50–100). Paleocurrent observations are more variable than for channelized sedimentary bodies and range from 230° to 150° (Fig. 6). This architecture is characterized by thick (to 12 m) packages of amalgamated sandstone (FA1) that laterally transition to nonamalgamated thick-bedded sandstone (FA2), and then back to FA1 (Fig. 8). Thus, the thicknesses of sandstone bodies increase and decrease considerably across the length of the outcrop belt, resulting in boudinage-like cross-sectional geometry. The top surface is generally flat, whereas the basal surface is undulatory and associated with truncation of underlying strata. The thickest, most amalgamated portions of these sedimentary bodies are present in concave-up depressions (Figs. 5 and 8). In some instances, beds infilling these depressions can be traced for ~1.5 km along strike. In the dip-oriented portion of the outcrop, these units thin and pinch out distally (Fig. 5). The lenticular sedimentary body architecture is pervasive in unit B and to a lesser degree in unit C (Figs. 5 and 6).

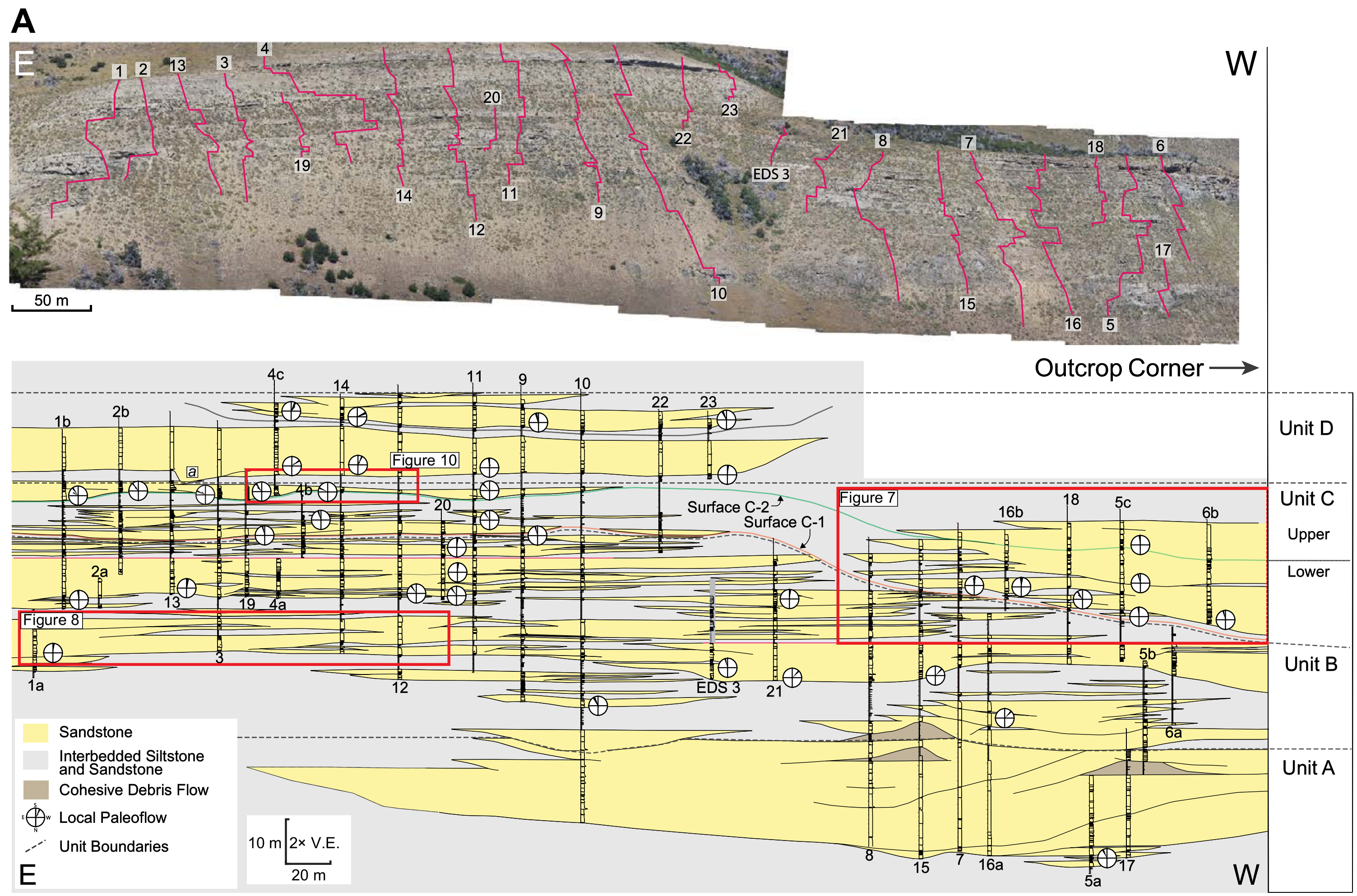

Figure 5 (*on this and following page*). Stratigraphic cross section of the Tres Pasos Formation outcrop at Arroyo Picana. The datum is on the top of major sandstone bodies. Average paleoflow is southward, shown with measurements summarized in rose diagrams. (A) The outcrop is generally at a slightly oblique strike orientation in the east-west section. V.E.—vertical exaggeration.

Interpretation. This architecture is interpreted to record the sandy infill of scour fields, such as those attributed to flow regime transition where entrainment is enhanced (Fig. 9) (Mutti and Normark, 1987). Scours can be isolated or coalesced, associated with rugosity in the depositional profile; if filled by sand, lenticular sedimentary body geometry is expected (e.g., Normark and Piper, 1991; Vicente Bravo and Robles, 1995; Wynn et al., 2002; Ito et al., 2014). Scour fields have been observed in channel-lobe transition zones and weakly confined channel settings using side-scan sonar imagery, with cross-sectional morphology comparable to that of the preserved basal surface in the outcrop belt (cf. Normark et al., 1979; Wynn et al., 2002; Maier et al., 2013). Drawing on these examples with similar cross-sectional geometry, and with consideration of the 2-D to 3-D exposure of units at Arroyo Picana, we infer original heel-shaped or flute-like morphology for these sedimentary bodies (cf. Wynn et al., 2002; Palanques et al., 1995; Macdonald et al., 2011; Maier et al., 2013; Hofstra et al., 2015). The thickest and coarsest grained portion of the bodies are attributed to processes in the axes of scours; correspondingly, the lateral bed thinning and

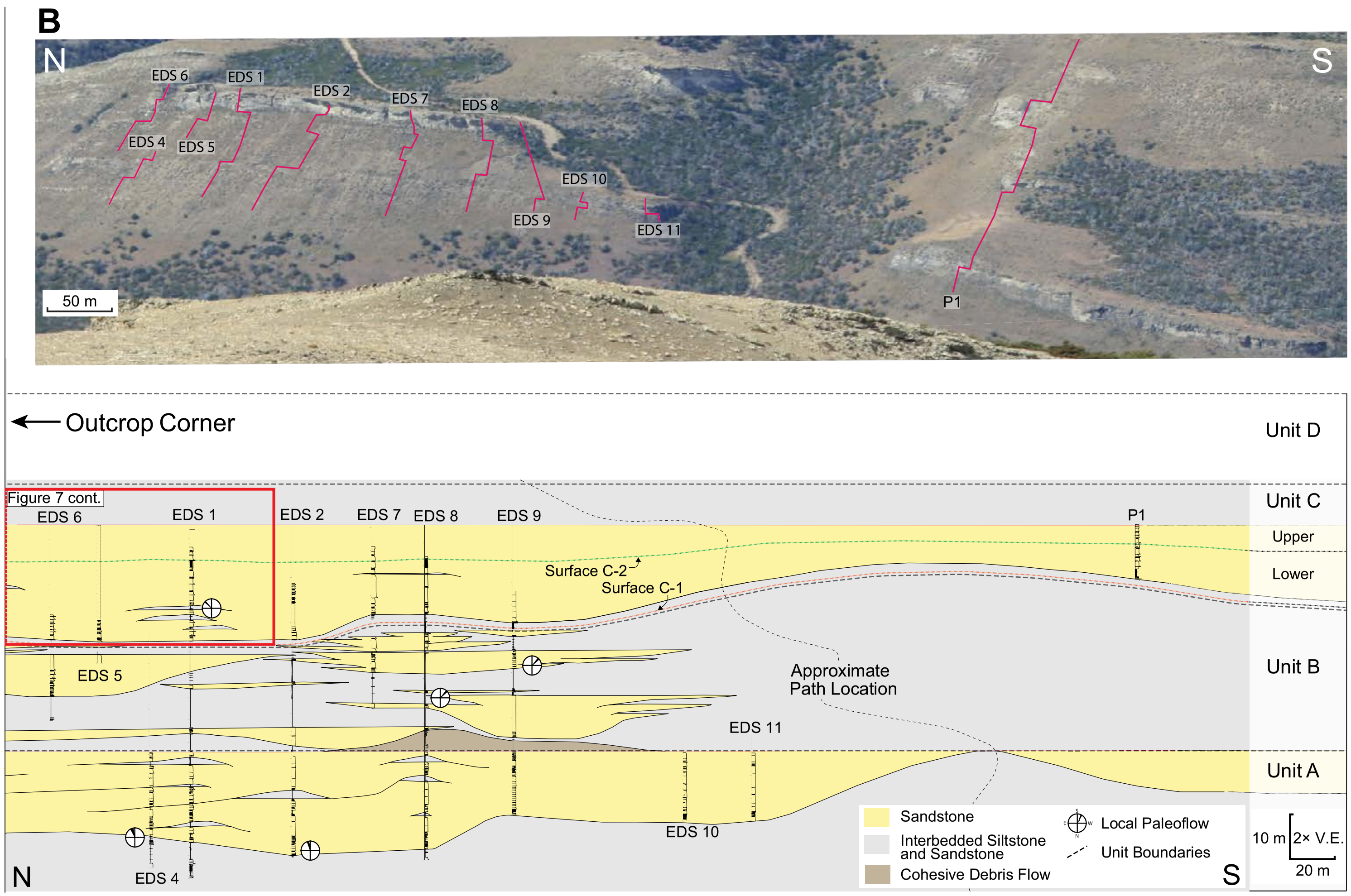

Figure 5 (*continued*). (B) The outcrop provides more of a dip perspective in the north-south section.

transition to nonamalgamated sandstone beds is associated with lower energy off-axis to margin processes (Wynn et al., 2002; McHargue et al., 2011; Macdonald et al., 2011). In general, coalesced scours, or scour complexes like those interpreted, have been reported at abrupt breaks in slope (Wynn et al., 2002).

Discontinuous Channelform Architecture

Description. In strike section, discontinuous channelform bodies are 0.5–6 m thick and 12–250 m wide, associated with aspect ratios between 20 and 30 (Fig. 5). Amalgamated sandstone (FA1) is dominant, although locally it transitions to nonamalgamated, thick-bedded sandstone (FA2) near the edges of the channelform; in some instances, an entire sedimentary body is composed of FA2. Basal surfaces of these bodies are associated with truncation of underlying strata, and the tops are flat. These sedimentary bodies are typically only exposed on a single outcrop face (Figs. 5 and 6), suggesting that they are isolated features; the largest discontinuous channelform sedimentary bodies are exposed on both strike and dip outcrop faces, and substantially thin at their base in the direction of paleoflow (Fig. 5). These sedimentary bodies are mainly observed in unit C with local expressions in units B and D (Fig. 7).

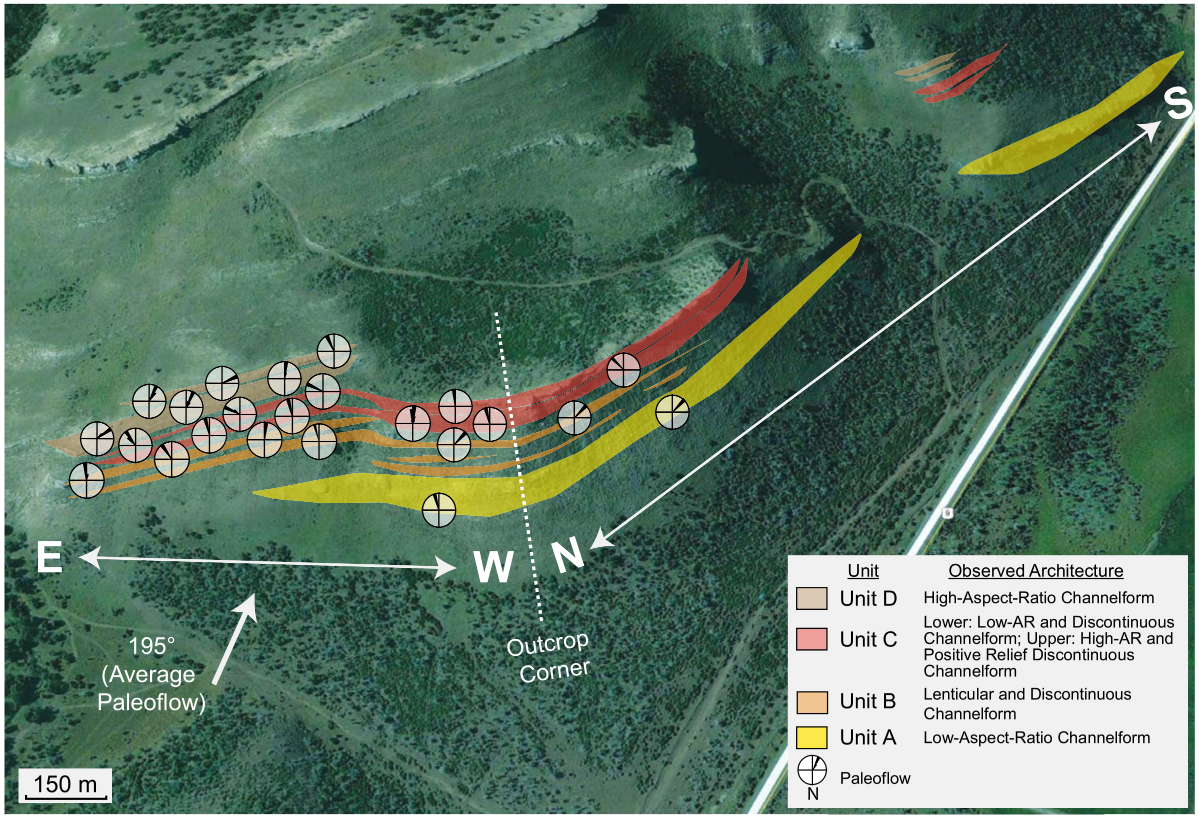

Figure 6. Perspective satellite image of the Arroyo Picana outcrop (highway at bottom right) highlighting the east-west–and north-south–oriented outcrop faces (Fig. 5); major stratigraphic units are highlighted (image courtesy of Google Earth). Our units (A–D) are delineated. Paleoflow directions for each unit are denoted by rose diagrams; the average paleoflow for the entire section is 195°, or roughly southward. AR—aspect ratio.

Interpretation. From 2-D and limited 3-D perspectives, these sedimentary bodies are elongate with scour-like geometries, and are attributed to turbidity current flow expansion across a transition zone associated with an abrupt decrease in confinement (cf. Normark and Piper, 1991). The cross-sectional shape of the bodies is similar to that of scours observed on the modern seafloor of continental slopes (e.g., Palanques et al., 1995; Wynn et al., 2002; Paull et al., 2010), and the 3-D planform insight drawn from these modern analogues suggests a heel- or flute-shaped planform morphology.

Cross-Stratified Positive-Relief Sedimentary Body Architecture

Description. A cross-stratified positive-relief sedimentary body 1–4.5 m thick is partially contained within depressions 55–135 m across and with as much as 0.9 m relief (Figs. 5 and 10). The depressions are aligned along the outcrop face at a bearing of ~100°E, which is parallel to the approximate direction of paleoflow, as derived from flute casts (102°–135°; Fig. 10). Nonamalgamated thick-bedded sandstone (FA2) is the dominant lithofacies of the infilling sedimentary body; sandstone is cross-stratified, with stratification dipping 7°–13° to the north. The top of the body expresses positive relief, and stratification in the upper portion is parallel to the overlying, undulatory bed top (Fig. 10). Packages of laminae can be traced into a sigmoid geometry, where at the tips and tails of the body laminae are more planar (Fig. 10). The cross-stratified body is present lateral to low-aspect-ratio channel fill of unit C, and is interpreted to overlie the same composite erosion surface (surface C-2; Fig. 5).

Interpretation. The cross-stratification dips in the opposite direction of paleoflow and the unit is interpreted as a positive-relief bedform feature that was instigated through backfilling of a scour on the seafloor (Postma et al., 2014). The position of this feature lateral to the low-aspect-ratio channel fill is consistent with an interpretation that it formed in a channel-flank setting (Figs. 5 and 10). Divergent paleoflow between the channel fill (~180°) and channel flank (102°–135°; Fig. 5) is consistent with lateral flow expansion as confinement

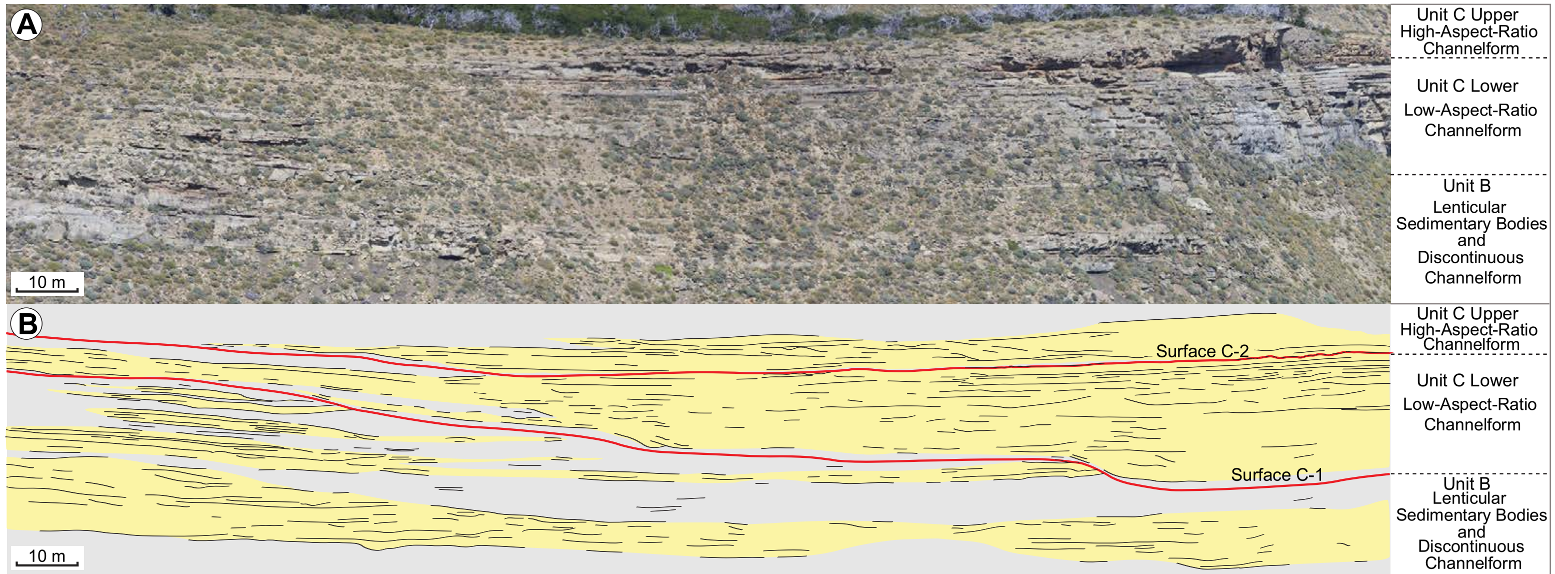

Figure 7. Channelized stratigraphic architecture. (A) Photomosaic of two channel elements in unit C, each defined by a fine-grained incisional surface (red). The lower element is as much as 19.6 m thick, and the upper element is 8.7 m thick. Photomosaic location is shown in Figure 5. (B) Line drawing trace.

was overcome. Flow transitions in overbank settings can manifest in the form of linear scour trains, termed cyclic steps (Parker, 1996; Kostic and Parker, 2006; Fildani et al., 2006). In these instances, each step is defined by an abrupt decrease in supercritical flow bounded downstream by a hydraulic jump; this yields formation of upslope-propagating bedforms that fill scours (Parker, 1996; Fildani et al., 2006; Cartigny et al., 2011; Macdonald et al., 2011). Although the scale of the series of depressions (i.e., scours) and the bedform described along surface C-2 (Fig. 5) is smaller than those recently described from seafloor and modeling data sets, we consider that the sedimentary body architecture may be a record of supercritical flow, with back-set cross-stratification indicative of antidunes (Middleton, 1965; Pickering et al., 2001) or, more likely, the expression of cyclic steps (Kostic, 2011; Covault et al., 2014; Postma et al., 2014).

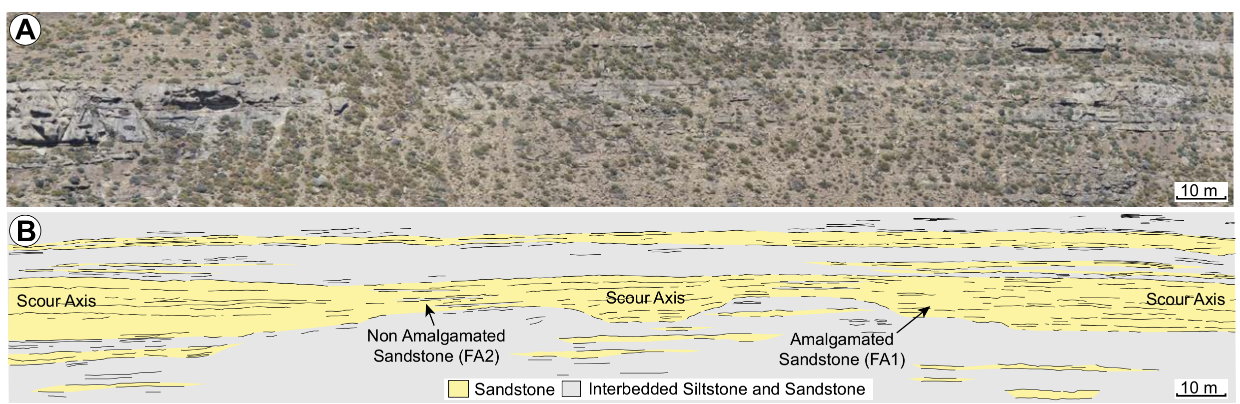

Figure 8. Lenticular sedimentary body architecture in unit B. (A) Photomosaic of amalgamated sandstone bodies (3–8 m thick) that thin and transition to nonamalgamated beds laterally. Photomosaic location is shown in Figure 5. (B) Line drawing trace.

Depositional Evolution

The sedimentary facies and architectural elements described suggest a depositional setting variably transitioning between confined, channelized flow and a less confined setting. The juxtaposition of various distinct architectural elements is consistent with a locality in which sediment transport processes and flow regimes changed rapidly, both spatially and temporally. Here we describe the depositional evolution of the strata at Arroyo Picana in the context of the four mapped stratigraphic packages (units A to D; Fig. 11).

Unit A

Unit A is dominated by low-aspect-ratio channelform sedimentary bodies; at least four separate channel elements (cf. Hubbard et al., 2014), defined locally by a basal surface draped by fine-grained deposits, vertically aggrade and laterally step to the southeast (Fig. 11). The channel-fill deposit is dominated by structureless sandstone with local contorted bedding and water escape features (FA4; Fig. 4). This composite sandstone-rich unit is mapped along the west face of the outcrop belt, and its eastern edge is present in three locations (Fig. 6), constraining its planform extent (Fig. 11).

This unit is considered an organized turbidite channel complex consisting of a series of channel fills that systematically shifted southeastward (cf. McHargue et al., 2011).

Unit B

Unit B is characterized by heterogeneous deposits, defined at the base by a lenticular sedimentary body that extends across the entire outcrop (individual beds can be traced 1.5 km; Fig. 11). This lenticular sandstone-prone architecture does not appear to correlate across the modern erosional valley, 250 m to the north (Fig. 2B), suggesting that the sandstone bodies are not continuous along depositional dip, but occur within a limited zone along the paleodepositional profile (Fig. 6). Between lenticular sedimentary bodies, more isolated discontinuous channelform sedimentary bodies are present (Fig. 11). This unit is present along the east-west face of the outcrop in a strike orientation and projected using paleoflow data; the planform extent of sedimentary bodies is constrained on the north-south–oriented outcrop face (i.e., dip orientation), which exhibits distinct thinning (Fig. 11).

The prevalence of lenticular sedimentary body geometries along with isolated discontinuous channel fills is consistent with observations of modern flow transition zones where large-scale scours commonly develop (Mutti and Normark, 1991; Wynn et al., 2002; Macdonald et al., 2011; Maier et al., 2012; Hofstra et al., 2015). The scours in these zones, including channel to lobe and confined channel to weakly confined channel intraslope transition zones, often coalesce and carve the seafloor into an undulatory surface. Infilling with sand results in

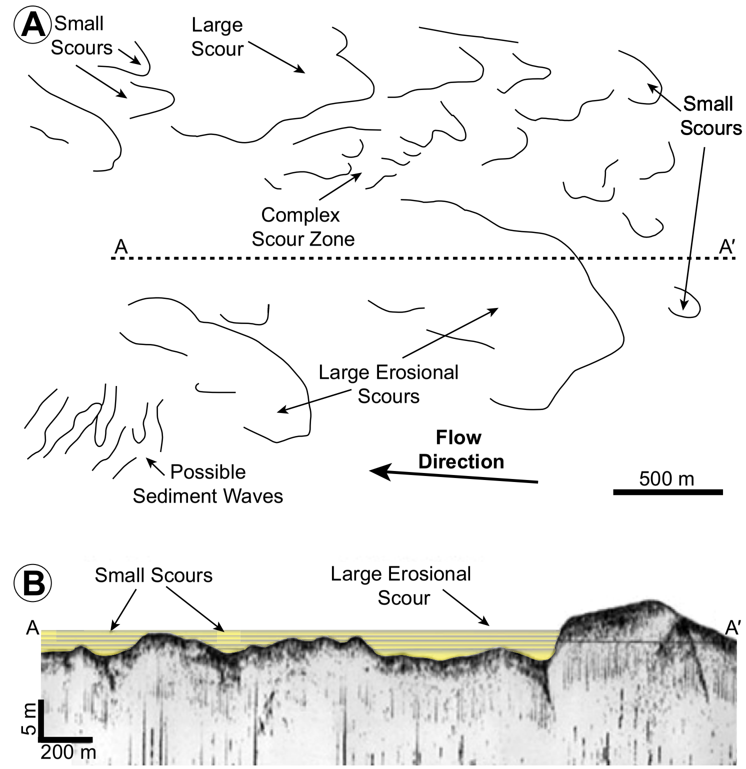

Figure 9. Characteristics of the Rhone fan channel-lobe transition zone (CLTZ) (modified from Wynn et al., 2002). (A) Line drawing from side-scan sonar image of the CLTZ. (B) Shallow seismic cross section (A–A′) through the CLTZ showing the undulatory nature of the seafloor in this zone. Yellow shading indicates how filling this zone may result in a high-aspect-ratio lenticular sedimentary body architecture like that observed in outcrop (Fig. 8; unit B).

the composite high-aspect-ratio sedimentary body documented (Fig. 9). If scours do not coalesce, more isolated discontinuous channelform bodies with flute-like scour planforms result (Fig. 11; cf. Wynn et al., 2002; Macdonald et al., 2011).

The 3-D mapping and projection of scour fills in the outcrop belt (Fig. 11) has relied on consideration and comparison of the sedimentary bodies documented with bathymetrically surveyed scours (Fig. 12). Using published overbank and channel-lobe transition zone metrics (i.e., scour width, length, depth, aspect ratio, and width:length ratio), regression curves were calculated. Given the limited 3-D outcrop exposure, these data were used to provide constraints on planform projection of sedimentary bodies. While additional scour data are available, only examples with lengths, widths, and depths were considered. These data indicate a trend that channel flank and/or overbank scours are generally wider than they are long, and scours found in channel-lobe

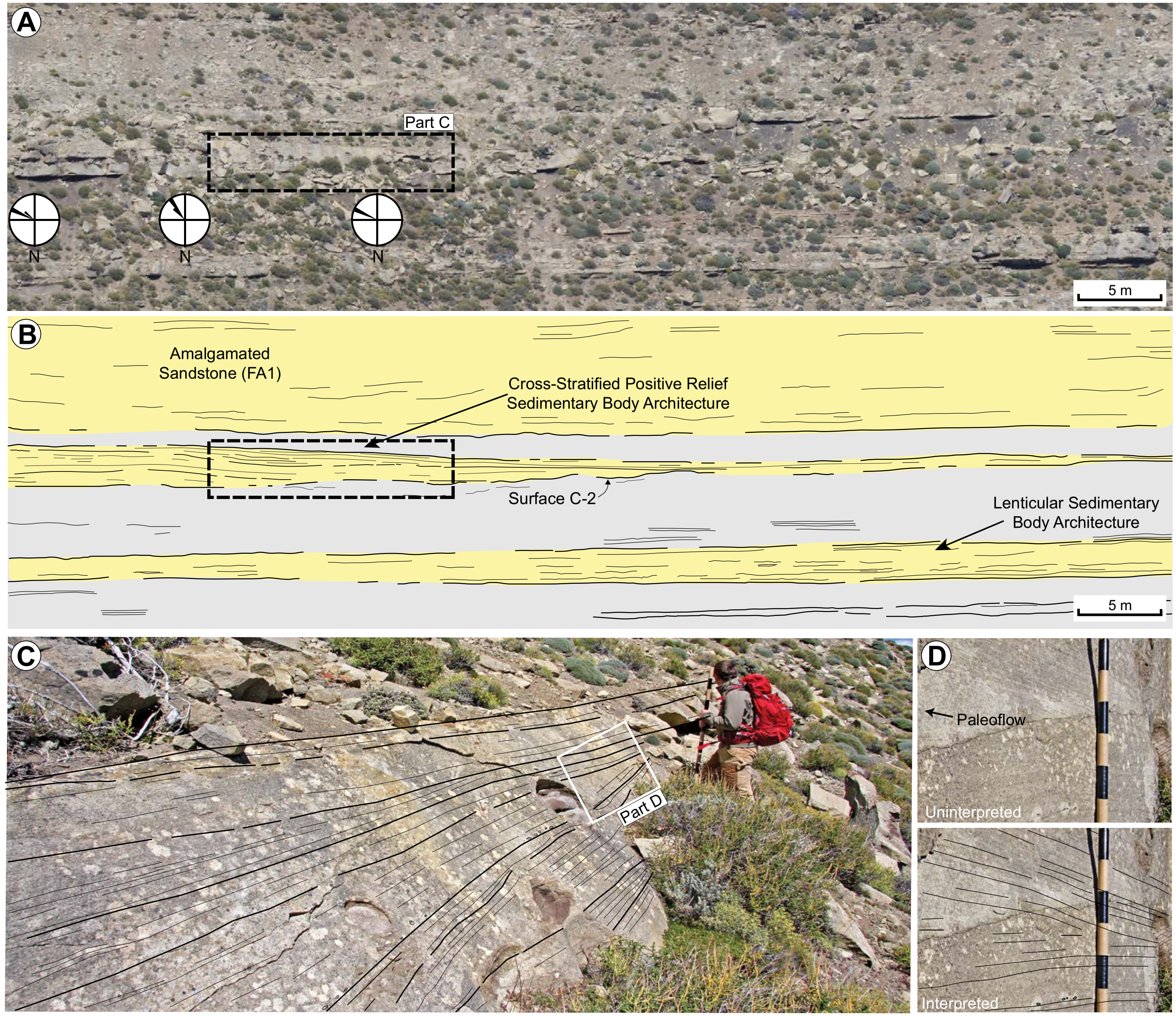

Figure 10. Cross-stratified positive-relief sedimentary body. (A) Photomosaic. (B) Line-drawing trace; dashed box highlights area in C. Paleoflow from flute casts is southward, although cross-sets dip northward. The location of this photomosaic is shown in Figure 5. (C) Closeup perspective showing the abrupt thinning of the sandstone in the distance (to the west). Laminae within the upper portion of this bed follow the upper relief of the bed, and are more horizontal toward the base. (D) Detail of cross-stratification.

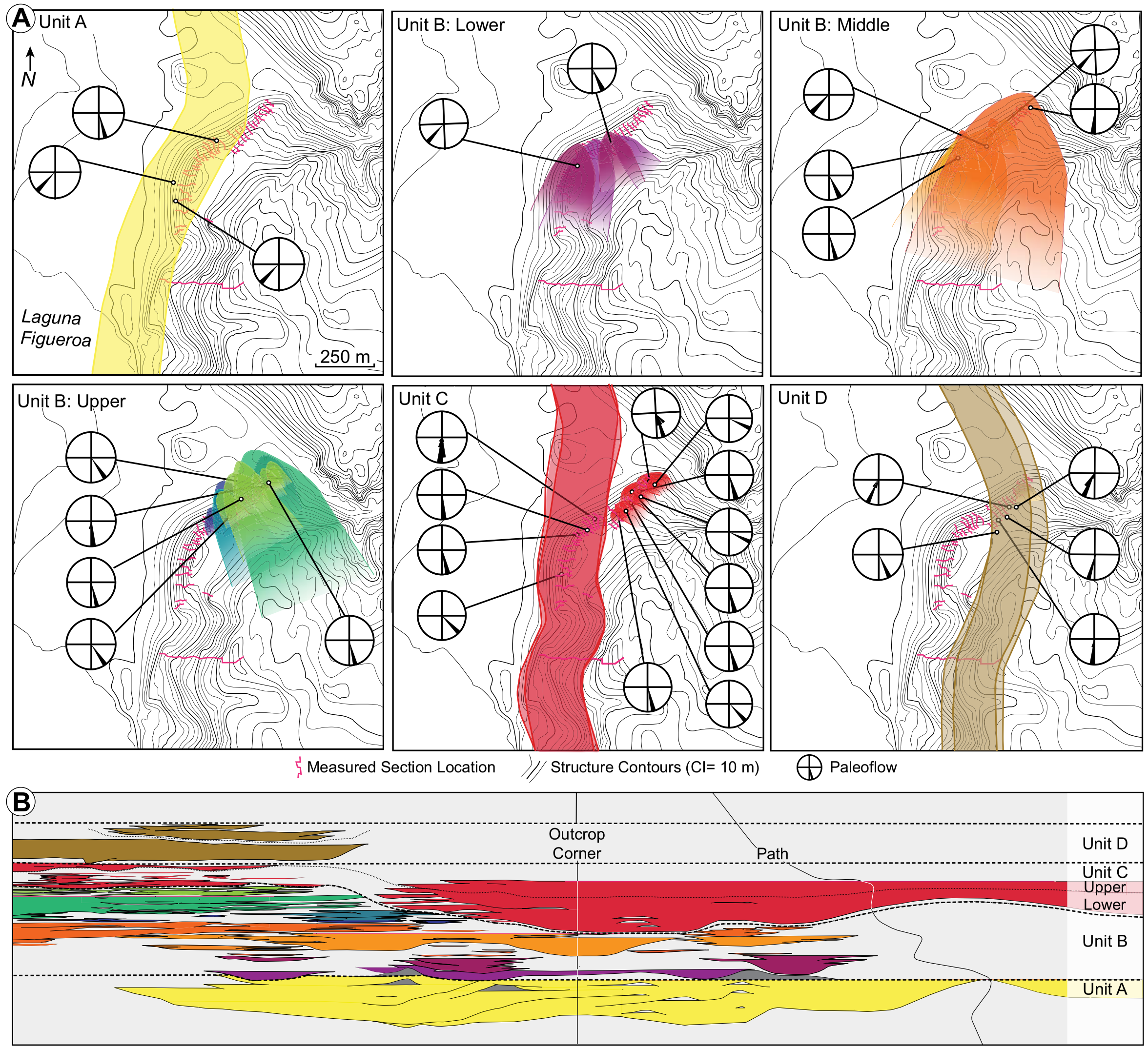

Figure 11. (A) Plan-view reconstructions of sedimentary bodies in each unit were generated by extrapolating outcrop data and flow axis trajectories over the entire study area. The analysis was guided by three-dimensional exposure, where possible, differential global positioning system–surveyed surfaces, paleoflow measurements, and insights from measurements of scours from modern seafloor data (Fig. 12). (B) Arroyo Picana outcrop stratigraphic cross section, modified from Figure 5, color coded by unit and corresponding to plan view diagrams in A. CI—contour interval.

transition zones are generally longer than they are wide (Figs. 11 and 12). Due to these differences in scour scale and geometry, and presumed differences in formative flow parameters, interpreted channel-lobe transition zone scour metrics were plotted separately from interpreted channel flank and/or overbank scour metrics (Fig. 12). We attribute the differences to the propensity for only the upper fraction of a turbidity current to detach from the main flow body in overbank settings (cf. Piper and Normark, 1983; Bowen et al., 1984), versus a channel-lobe transition zone where the entire flow thickness (including the lower, high-density component) goes through deceleration (Normark and Piper, 1983; Clark and Pickering, 1996). High-density turbidity currents have a much thicker tractional component than low-density flows (Lowe, 1982), and we speculate that subjecting this entire flow thickness to transformation across a hydraulic jump may lead to development of scours that are generally longer than they are wide (Figs. 11 and 12).

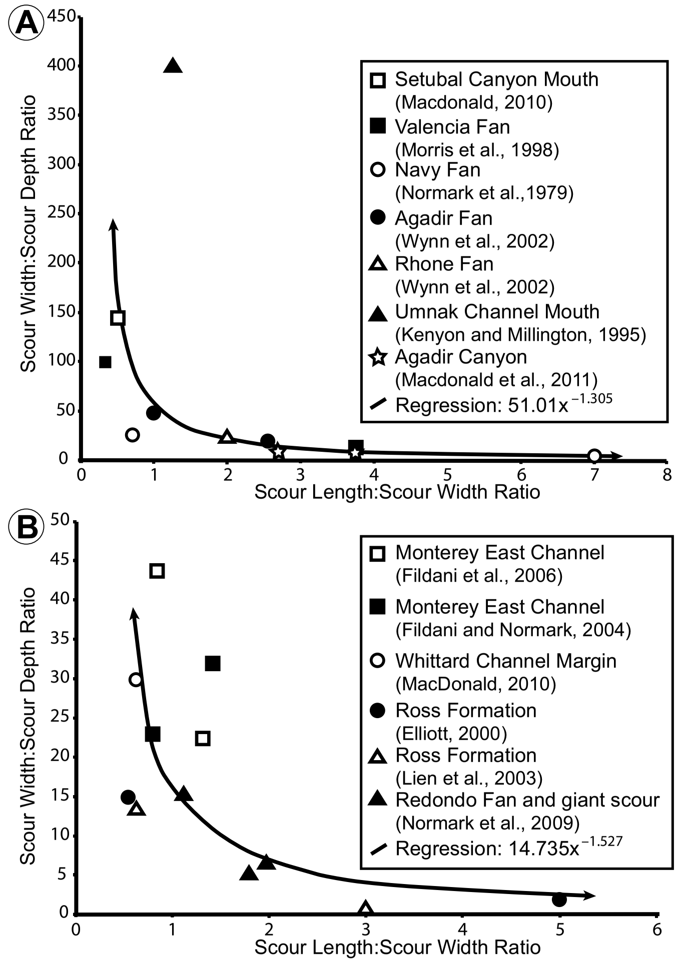

Figure 12. Regression curves of scour sizes and geometries. (A) From channel-lobe transition zones. (B) From channel overbank settings. These data were used to extrapolate scourform dimensions and extents in the outcrop belt where exposure was limited.

Unit C

Unit C is composed of two channel fills and adjacent heterogeneous deposits (Figs. 5, 7, and 10). A lower low-aspect-ratio channelform sedimentary body is as much as 19.6 m thick, defined by a distinctive and laterally continuous (>1 m thick) channel base drape overlying surface C-1 (Figs. 5 and 7). An upper high-aspect-ratio channelform sedimentary body is much thinner (8.7 m thick) and shallower, with a higher aspect ratio of ~54 (Fig. 11); it is also defined at its base by a siltstone drape overlying surface C-2 (Figs. 5 and 7). To the east, laterally flanking the channel-fill elements and overlying consistent basal erosional surfaces (C-1 and C-2; Fig. 5), are small-scale discontinuous architectural elements ~30–270 m wide and 0.6–4.6 m thick (Fig. 11). The lower channel fill is associated laterally with isolated discontinuous channelform bodies that are infilled mainly with structureless sandstone, while the upper channel element is associated laterally with cross-stratified positive-relief bodies (Figs. 5 and 11). These small-scale architectural elements are not observed northward across the Arroyo Picana valley, although the eastern margins of the larger channel fills are present (Fig. 11). The continuous downdip exposure of these two channel fills along the west-facing outcrop, as well as multiple exposures of their eastern margins at the southern end of the outcrop belt, constrain the 3-D interpretation of the units (Fig. 11).

The architectural components of unit C are attributed to turbidite slope channel elements and laterally flanking out-of-channel deposits. The vertically stacked channel fills suggest that the underlying channel was underfilled upon abandonment, and was therefore the locus for subsequent channelization (cf. McHargue et al., 2011). Laterally flanking the channel fills of unit C, the small-scale scourform features are interpreted to have formed in response to rapid flow regime transition as flows overspilled channel banks (cf. Normark and Piper, 1991; Vicente Bravo and Robles, 1995; Fildani and Normark, 2004). Consistent with this interpretation, the out-of-channel elements are composed of slightly reduced average grain size relative to the channel fills they flank. The cross-stratified positive-relief body is characterized by paleoflow that is divergent from that of the associated channel element (Fig. 11); back-set cross-stratification is consistent with antidunes or cyclic steps (Pickering et al., 2001; Kostic, 2011; Cartigny et al., 2013).

Unit D

Unit D is characterized by two high-aspect-ratio (~50) channelform bodies at the eastern edge of the outcrop exposure (Figs. 7 and 11). Although generally defined by smooth, concave-up bases, the lower element is characterized by a distinct protuberance that is interpreted as the remnant of a scour (Fig. 5A, feature a). The scour is ~30 m wide and 3 m deep, overlain by channel-fill deposits across a truncation surface. The 3-D exposure of unit D is limited, making planform reconstructions highly speculative (Fig. 11). Unit D is overlain by ~22 m of interbedded siltstone and sandstone (FA3).

Unit D comprises weakly confined channel deposits (cf. McHargue et al., 2011; Moody et al., 2012; Brunt et al., 2013). Weakly confined channel systems are interpreted in a range of settings and are generally found in topographic lows, areas with low slope, or base-of-slope settings (e.g., Campion et al., 2005; Maier et al., 2011; Moody et al., 2012). The localized scour fill described at the base of the unit D channel fill is geometrically comparable in strike section to geomorphological features described from turbidite channel and canyon floors in modern seafloor data, albeit at a reduced scale (Paull et al., 2010, 2011; Cartigny et al., 2011; Maier et al., 2011, 2013; Covault et al., 2014).

DISCUSSION

Slope Channel Evolution

The Cretaceous Magallanes Basin margin was dominated by high sedimentation, recorded by a prograding slope clinoform system (Hubbard et al., 2010; Romans et al., 2011). Enhanced aggradation of sediment on the paleoslope yielded a particularly thick stratigraphic record of the sediment-routing system studied, ideal for deducing information about long-lived sedimentary processes. The outcrop at Arroyo Picana shows variable stratigraphic architecture within ~100 m of stratigraphic thickness (Fig. 5). Recent analysis of seafloor data from offshore central California presented by Maier et al. (2011, 2013; Fig. 13) highlighted geomorphic variations over a fairly limited area, including leveed channels, broad erosional channels, and trains of scours, recording slope channels at various evolutionary stages. We consider the possibility that the various architectural components present in the Arroyo Picana outcrop might record turbidite channels preserved at various stages of development.

Our hypothesis is that discontinuous channelform features (i.e., scours) evolve into high-aspect-ratio continuous channelform sedimentary bodies (i.e., weakly confined channels), and under the influence of protracted flow, into low-aspect-ratio continuous channelform features (i.e., confined slope channels; Figs. 13 and 14).

Discontinuous Channelform Architecture

Discontinuous channelform bodies, such as those prevalent in unit B, are interpreted to record an early evolutionary stage of a turbidite channel (Figs. 8 and 14). Previous workers have considered morphological features with a similar shape at the base of these stratigraphic bodies as evidence for incipient channels from analysis of modern acoustic data sets (e.g., Fildani and Normark, 2004; Fildani et al., 2006; Maier et al., 2011, 2013). Large scours have been recognized within continuous channels or conduits (cf. Paull et al., 2011), downslope, and in the direction, of continuous channels (Figs. 13 and 14), as well as in overbank areas associated with through-going continuous channels (e.g., Monterey East; Fildani and Normark, 2004; Fildani et al., 2006). The initial erosional stage of a conduit and the establishment of an erosional template was proposed by Rowland et al. (2010) based on experimental data. This initial erosion has been proposed to facilitate the inception of locked-in-place linear trains of discontinuous scours or net-erosional cyclic steps (Figs. 11 and 14). The erosional confinement created is thought to focus subsequent flows, often related to an upslope avulsion node (Fig. 13; Maier et al., 2011, 2012; Fildani et al., 2013). As flows continue along the trajectory, the discontinuous train of scours will eventually connect and confinement will develop; a more continuous low-aspect-ratio channel will form (Fig. 14, stage 1b; Deptuck et al., 2003; Hughes Clarke et al., 2013; Covault et al., 2014).

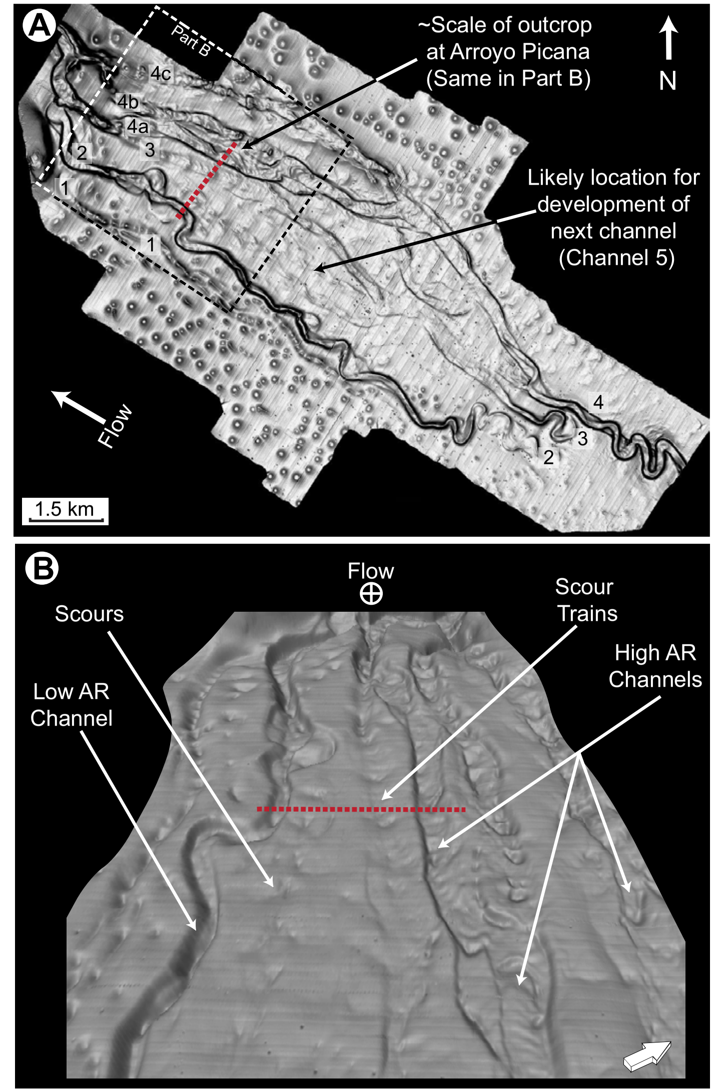

Figure 13. Autonomous underwater vehicle multibeam bathymetric data from Lucia Chica, California. (A) Shaded relief image (4× vertical exaggeration) of the data set with main channel bodies numbered in sequence by relative age and sequence of avulsion (modified from Maier et al., 2013). The dashed line rectangle delineates the area of the perspective image in B and the red dashed line indicates the approximate scale of the Tres Pasos Formation outcrop at Arroyo Picana (same scale in B). This red line intersects various architectural elements in close proximity both laterally and vertically, similar to what is preserved at Arroyo Picana. (B) Perspective image of multibeam bathymetric data; low-aspect-ratio channels, high-aspect-ratio channels, scours, and linear trains of scours are present in this data set, at roughly the scale of the outcrop at Arroyo Picana.

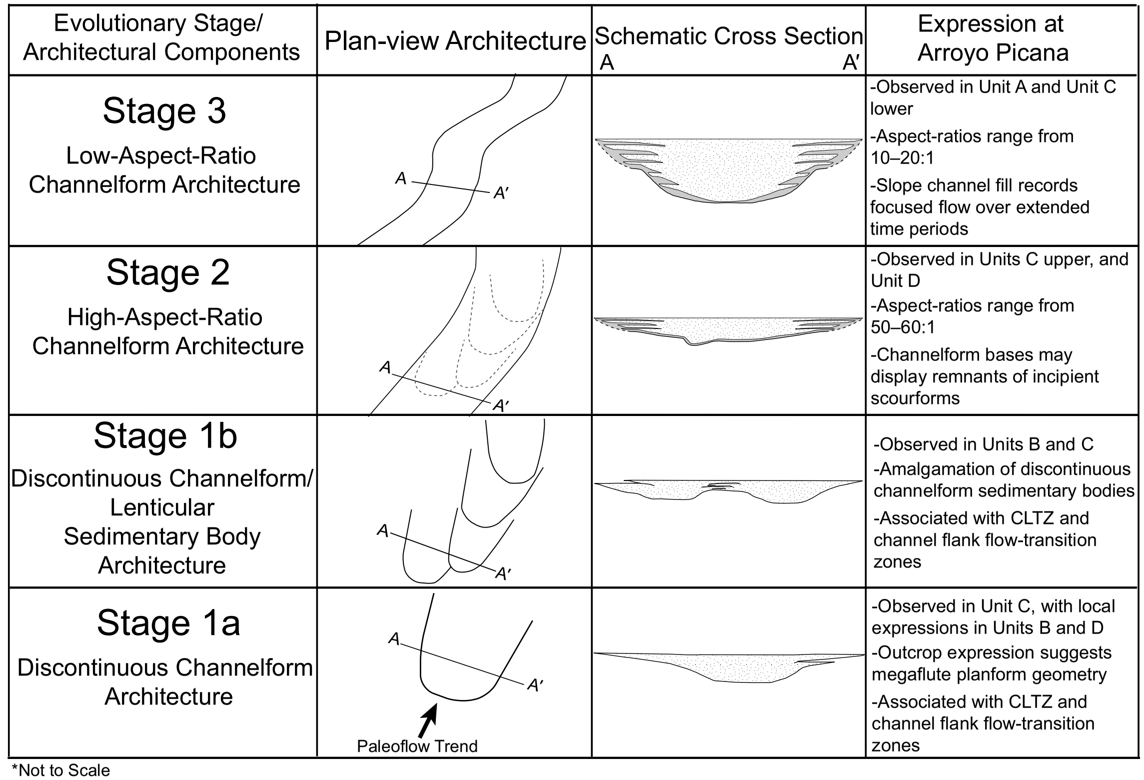

Figure 14. Proposed evolution of turbidite channels as observed from architectural components present in the Arroyo Picana outcrop. Stage 1 is characterized by discontinuous channelform architecture, attributed to scour erosion on the seafloor; a series of these features can result in formation of a train of scours, which act to capture subsequent flows (cf. Fildani et al., 2013). This leads to stage 2, where flows are focused for long enough to establish a broad and shallow conduit, which may or may not display remnants of scourform features at its base. The focus of numerous flows through these channels can result in formation of deeper, low-aspect-ratio channels (Stage 3). CLTZ—channel-lobe transition zone.

The fills of numerous scours can be interpreted from the Arroyo Picana outcrop, including numerous large-scale coalesced scours (unit B, Fig. 11). The remnant of a scour beneath the high-aspect-ratio channel fill in lower unit D (Fig. 5A, feature a) and the similarity in amalgamated sandstone (FA1) in both the scour and overlying channel fill suggest that the scour was eroded into the seafloor prior to subsequent formation of the through-going channel.

High-Aspect-Ratio Channelform Architecture

High-aspect-ratio channelform bodies are considered to represent a subsequent stage of turbidite channel evolution (Fig. 14; cf. Fildani et al., 2006, 2013; Maier et al., 2011, 2012). If flows are focused for long enough through scour trains or bathymetric depressions, a low-relief channel (weakly confined) is postulated to develop (represented by the high-aspect-ratio channelform architecture of unit D). Often low-relief turbidite channels cannot keep entire flows confined, and therefore the tendency is for them to breach confinement and expand, often leaving behind deposits on the overbank or flank of the channel (Maier et al., 2013; Stevenson et al., 2013). This type of channel can be prone to avulsion, until a deeper channel is established (Maier et al., 2011, 2013; McHargue et al., 2011). If a deep low-aspect-ratio channel does not develop, the weakly confined channels may be abandoned and left underfilled by coarse sediment as a result of updip avulsion (Maier et al., 2011, 2012; Stevenson et al., 2013). The Lucia Chica channel system shows that the youngest channels are broad (high-aspect-ratio) and either have no levees or have low-relief levees; in addition, aligned flute-shaped erosional depressions are observed in the bases of these features (Fig. 13; Maier et al., 2013; Fildani et al., 2013). We propose that this results in a stratigraphic framework similar to that preserved in units C and D at the Arroyo Picana outcrop (Fig. 11). Although coeval lobe deposits are not exposed in the outcrop belt documented here, similar shallow and broad channels are located immediately updip of lobes in other outcrop belts (e.g., Karoo Basin; Prélat et al., 2009; Morris et al., 2014; Van der Merwe et al., 2014).

Low-Aspect-Ratio Channelform Architecture

The final stage in turbidite channel evolution is preserved by the low-aspect-ratio continuous channelform architecture prominent in unit C (Figs. 7 and 14). This architectural element is described from outcrops (e.g., Mutti and Normark, 1987; Beaubouef et al., 1999; Gardner et al., 2003; Campion et al., 2005; Pyles et al., 2010; Macauley and Hubbard, 2013) and other data sets (e.g., McHargue et al., 2011; Maier et al., 2012; Jobe et al., 2015). This style of channel architecture was described from overlying units of the Tres Pasos Formation (Hubbard et al., 2014), emphasizing evidence for innumerable turbidity currents that passed through the channel over its lifespan, recorded in fine-grained basal and marginal facies, as well as massive and amalgamated sandstone fill. In Hubbard et al. (2014) evidence for sediment bypass, underfit flows (i.e., flows smaller than their conduits), multiple phases of incision, and collapsing turbidity currents from intrachannel fill observations was emphasized. The stratigraphy that overlies the Arroyo Picana outcrop (directly overlying unit D; Figs. 2B–2D) consists of ~330 m of dominantly low-aspect-ratio channelform bodies (Hubbard et al., 2010, 2014; Macauley and Hubbard, 2013).

Stratigraphic and Geomorphologic Surfaces

Numerous large turbidity flows are considered to initiate and drive erosion of slope channels (e.g., Elliott, 2000; Pirmez et al., 2000; Gee et al., 2007; Hodgson et al., 2011; Fildani et al., 2013). Channel maintenance, including mass wasting of channel margins, erosion, and sediment bypass, is prevalent throughout much of the channel lifecycle (Covault et al., 2014; Hubbard et al., 2014; Stevenson et al., 2015). Overspill of sediment into channel-overbank areas results in levee construction, which contributes to confinement of successive flows (Mutti and Normark, 1987; Flood et al., 1995; Kane and Hodgson, 2011; McHargue et al., 2011; Maier et al., 2011). Phases of deposition in channels can be the result of insufficient flow energy, step drop in flow velocity across a hydraulic jump, ponding in response to modification of the equilibrium profile by emplacement of slumps, or decreased accommodation downslope and subsequent backfilling (e.g., Mutti and Normark, 1987; Clark and Pickering, 1996; Gardner and Borer, 2000; Postma et al., 2009; McHargue et al., 2011; Covault et al., 2014). Through this multiphase history of channelization, it is not surprising that channel fills are composite bodies bound by highly diachronous stratigraphic surfaces (Fig. 15). This evolution invariably leads to the generation of channelform-bounding stratigraphic surfaces that bear little resemblance to formative geomorphic surfaces that existed on the seafloor (Fig. 15; cf. Strong and Paola, 2008; DiCelma et al., 2011; Sylvester et al., 2011).

Despite the varied processes that contribute to the formation and filling of channels, protracted and focused flows lead to a product that is generally persistent and repeated globally (i.e., channel element fill of Mutti and Normark, 1987; Sullivan et al., 2000; Gardner et al., 2003; Pyles et al., 2010; McHargue et al., 2011; Hubbard et al., 2014). Furthermore, the stratigraphic stacking of successive channel elements can also be regular; for example, some channel fills consistently stack aggradationally with limited lateral offset due to levee or inner levee confinement and the disposition to being left underfilled upon abandonment (cf. McHargue et al., 2011).

We speculate that settings in which confined to less-confined flow transitions persist are associated with the elevated transfer of geomorphic surfaces to the stratigraphic record (Figs. 14 and 15). Unlike channels that form through

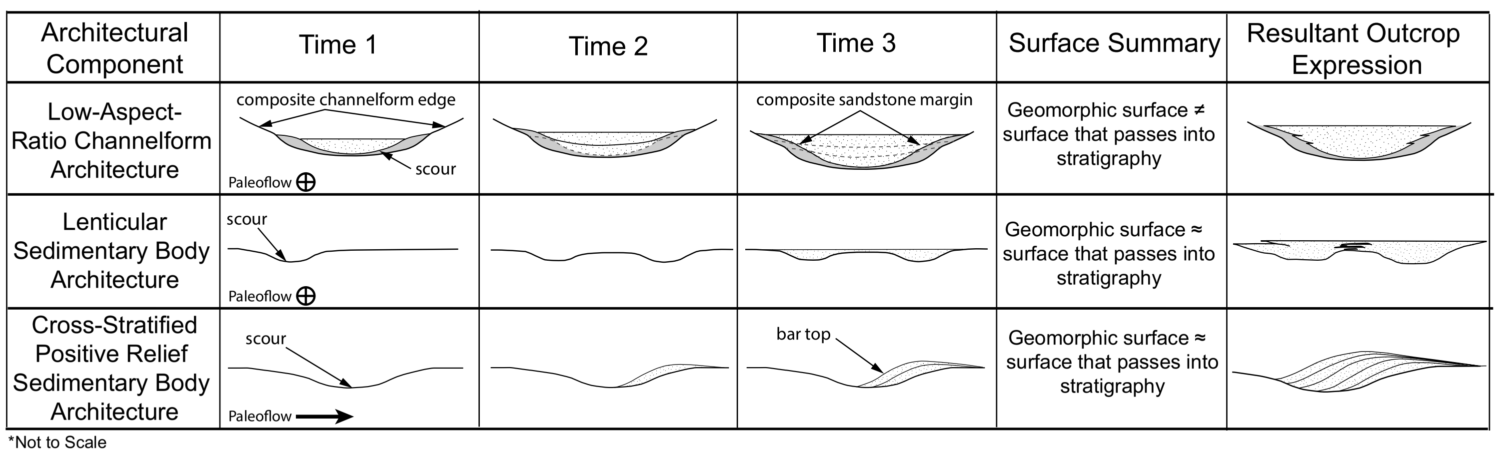

Figure 15. Examples of sedimentary body architecture preserved in the Arroyo Picana outcrop, with emphasis on the difference in geomorphic surfaces and the surfaces that pass through to the stratigraphic record.

numerous stages of focused incision and filling over a protracted period, evidence for this multistage history (e.g., intrachannel siltstone-draped scours, thin-bedded margin deposits; cf. Hubbard et al., 2014) is not present in most architectural elements of depositional zones where flow transitions occur (e.g., Figs. 8 and 9). A somewhat simpler, and abbreviated, history of erosion and sediment bypass followed by rapid backfilling of sands and burial enhances preservation potential of geomorphic surfaces. We speculate that transient features and patterns observable on the modern seafloor are potentially preserved in the stratigraphic record, but only under certain conditions. For example, regular avulsion of flow pathways in weakly confined to unconfined settings results in bathymetric and depositional features that are not as prone to cannibalization by subsequent deep incision and prolonged channel processes (Wynn et al., 2002; Macdonald et al., 2011). In the case of the Tres Pasos Formation, the high-aggradation net-depositional setting associated with the progradational basin margin resulted in burial, which favored preservation of the varied stratigraphic architecture, attributable to numerous stages of channel development (Fig. 14).

Repeated patterns of fill within and among sedimentary bodies have not been well established in the analysis of strata attributed to zones of flow transition (e.g., Cazzola et al., 1981; Mutti et al., 1985; Wynn et al., 2002; Gardner et al., 2003; Van der Merwe et al., 2014), in contrast to those of channel fills, which stem from a prevalence of focused flows over sustained periods (e.g., Deptuck et al., 2007; Maier et al., 2011; Fildani et al., 2013; Hubbard et al., 2014). The ephemeral nature, varied flow pathways, and limited erosion from subsequent channelization yield a more architecturally diverse and less predictable stratigraphic expression of the response to decreasing confinement that has historically been difficult to recognize, and therefore has been underreported.

CONCLUSIONS

Although the stratigraphic expression of long-lived submarine channel and lobe complexes are generally well established, the same cannot be said for the stratigraphic expression of transition zones between these segments of deep-sea sediment routing systems. The Cretaceous Tres Pasos Formation that crops out at Arroyo Picana in the Magallanes Basin, southernmost Chile, consists of varied architectural elements present in close association, including: (1) low-aspect-ratio slope channel fills; (2) high-aspect-ratio weakly confined channel fills; (3) lenticular, laterally amalgamated scour fills; (4) isolated scour fills; and (5) cross-stratified, migrating depositional bedform deposits. The strata are interpreted to contain the record of a decrease in channel confinement along the deep-water paleoslope.

Abundant evidence for scours and sediment bypass records a deep-water sediment routing system segment characterized by decreasing confinement, shifting flow pathways, and bathymetric irregularity. Unlike long-lived channel systems that tend to remain focused and thus cannibalize the record of formative processes at the expense of later erosion and deposition events, shifting flow pathways in less-confined settings combined with burial driven by high aggradation resulted in excellent preservation of sedimentary units. The Tres Pasos Formation outcrop preserves a unique perspective of turbidite channels at various stages of development, from early stage discontinuous and isolated scour fills to low-aspect-ratio channel-fill units. The diverse sedimentary units transferred into the rock record result in less regular stratigraphic patterns than those described from updip channel-dominated or downdip lobe-dominated units; this has negatively affected their recognition in other stratigraphic data sets.

ACKNOWLEDGMENTS

We thank Tamara McLeod and Jose Antonio Kusanovic for access to the outcrops in southern Chile. Students from the University of Calgary, including Sean Fletcher, Keegan Raines, Dallin Laycock, Dustin Bauer, Ryan Macauley, Ross Kukulski, Ben Daniels, and Aaron Reimchen, provided capable field assistance and/or enlightening discussion. Discussions with many colleagues, including Julian Clark, Kirt Campion and Bill Morris, contributed to our understanding of these depositional systems. Funding was generously provided from the Chile Slope Systems (CSS) joint industry project (Anadarko, BG Group, BHP Billiton, BP, Chevron, ConocoPhillips, Hess, Maersk, Marathon, Nexen, Shell, Statoil, and Talisman Energy). The clarity and quality of this manuscript was greatly improved by the insightful comments of Dave Hodgson and two anonymous reviewers.

REFERENCES CITED

Adeogba, A.A., McHargue, T.R., and Graham, S.A., 2005, Transient fan architecture and depositional controls from near-surface 3-D seismic data, Niger Delta continental slope: American Association of Petroleum Geologists Bulletin, v. 89, p. 627–643, doi: 10.1306/11200404025.

Barton, M., Byrne, C.O., Pirmez, C., Prather, B., van der Vlugt, F., Alpak, F.O., and Sylvester, Z., 2010, Turbidite channel architecture: Recognizing and quantifying the distribution of channel-base drapes using core and dipmeter data, *in* Pöppelreiter, M., et al., eds., Dipmeter and borehole image-log technology: American Association of Petroleum Geologists Memoir 92, p. 195–211, doi:10.1306/13181284M923289.

Bauer, D.B., 2012, Stratigraphic evolution of a high-relief slope clinoform system, Magallanes Basin, Chilean Patagonia [M.S. thesis]: Calgary, University of Calgary, 120 p.

Beaubouef, R.T., Rossen, C.R., Zelt, F.B., Sullivan, M.D., Mohrig, D.C., Jennette, D.C., Bellian, J.A., Friedman, S.J., Lovell, R.W., and Shannon, D.S., 1999, Deep-water sandstones, Brushy Canyon Formation, west Texas: American Association of Petroleum Geologists Continuing Education Course Note Series 40, 48 p.

Bouma, A.H., 1962, Sedimentology of some flysch deposits: A graphic approach to facies interpretation: Amsterdam, Elsevier, 168 p.

Bowen, A.J., Normark, W.R., and Piper, D.J., 1984, Modelling of turbidity currents on Navy Submarine Fan, California continental borderland: Sedimentology, v. 31, p. 169–185, doi:10.1111/j.1365-3091.1984.tb01957.x.

Brunt, R.L., Hodgson, D.M., Flint, S.S., Pringle, J.K., Di Celma, C., Prélat, A., and Grecula, M., 2013, Confined to unconfined: Anatomy of a base of slope succession, Karoo Basin, South Africa: Marine and Petroleum Geology, v. 41, p. 206–221, doi:10.1016/j.marpetgeo.2012.02.007.

Campion, K.M., Sprague, A.R., and Sullivan, M.D., 2005, Architecture and lithofacies of the Capistrano Formation (Miocene–Pliocene), San Clemente, California: Pacific Section, American Association of Petroleum Geologists Fieldtrip Guidebook 100, 42 p.

Cartigny, M.J.B., Postma, G., van den Berg, J.H., and Mastbergen, D.R., 2011, A comparative study of sediment waves and cyclic steps based on geometries, internal structures and numerical modeling: Marine Geology, v. 280, p. 40–56, doi:10.1016/j.margeo.2010.11.006.

Cartigny, M.J.B., Eggenhuisen, J.T., Hansen, E.W.M., and Postma, G., 2013, Concentration-dependent flow stratification in experimental high-density turbidity currents and their relevance to turbidite facies models: Journal of Sedimentary Research, v. 83, p. 1046–1064, doi:10.2110/jsr.2013.71.

Cazzola, C., Fonnesu, F., Mutti, E., Rampone, G., Sonnino, M., and Vigna, B., 1981, Geometry and facies of small, fault-controlled deep-sea fan systems in a transgressive depositional setting (Tertiary Piedmont basin, north-western Italy), *in* Ricci Lucchi, F., ed., 2nd European Regional Meeting 1981, Bologna, Italy: Excursion guidebook with contributions on sedimentology of some Italian basins: Bologna, Italy, International Association of Sedimentologists, p. 5–56.
Clark, J.D., and Pickering, K.T., 1996, Architectural elements and growth patterns of submarine channels: Application to hydrocarbon exploration: American Association of Petroleum Geologists Bulletin, v. 80, p. 194–221.
Covault, J.A., Kostic, S., Paull, C.K., Ryan, H.F., and Fildani, A., 2014, Submarine channel initiation, filling and maintenance from sea-floor geomorphology and morphodynamic modeling of cyclic steps: Sedimentology, v. 61, p. 1031–1054, doi:10.1111/sed.12084.
Daniels, B.G., 2015, Downslope characterization of channel fill and stratigraphic architecture along an ancient basin margin, Tres Pasos Formation, southern Chile [M.S. thesis]: Calgary, University of Calgary, 153 p.
Deptuck, M.E., Steffens, G.S., Barton, M., and Pirmez, C., 2003, Architecture and evolution of upper fan channel-belts on the Niger Delta slope and in the Arabian Sea: Marine and Petroleum Geology, v. 20, p. 649–676, doi:10.1016/j.marpetgeo.2003.01.004.
Deptuck, M.E., Sylvester, Z., Pirmez, C., and O'Byrne, C., 2007, Migration-aggradation history and 3-D seismic geomorphology of submarine channels in the Pleistocene Benin-major Canyon, western Niger Delta slope: Marine and Petroleum Geology, v. 24, p. 406–433, doi:10.1016/j.marpetgeo.2007.01.005.
Di Celma, C.N., Brunt, R.L., Hodgson, D.M., Flint, S.S., and Kavanagh, J.P., 2011, Spatial and temporal evolution of a Permian submarine slope channel-levee system, Karoo basin, South Africa: Journal of Sedimentary Research, v. 81, p. 579–599, doi:10.2110/jsr.2011.49.
Elliott, T., 2000, Megaflute erosion surfaces and the initiation of turbidite channels: Geology, v. 28, p. 119–122, doi:10.1130/0091-7613(2000)28<119:MESATI>2.0.CO;2.
Figueiredo, J.J.P., Hodgson, D.M., Flint, S.S., and Kavanagh, J.P., 2013, Architecture of a channel complex formed and filled during long-term degradation and entrenchment on the upper submarine slope, Unit F, Fort Brown Fm., SW Karoo Basin, South Africa: Marine and Petroleum Geology, v. 41, p. 104–116, doi:10.1016/j.marpetgeo.2012.02.006.
Fildani, A., and Hessler, A., 2005, Stratigraphic record across a retroarc foreland basin inversion: Rocas Verdes-Magallanes Basin, Patagonian Andes, Chile: Geological Society of America Bulletin, v. 117, p. 1596–1614, doi:10.1130/B25708.1.
Fildani, A., and Normark, W.R., 2004, Late Quaternary evolution of channel and lobe complexes of Monterey Fan: Marine Geology, v. 206, p. 199–223, doi:10.1016/j.margeo.2004.03.001.
Fildani, A., Normark, W.R., Kostic, S., and Parker, G., 2006, Channel formation by flow stripping: Large-scale scour features along the Monterey East Channel and their relation to sediment waves: Sedimentology, v. 53, p. 1265–1287, doi:10.1111/j.1365-3091.2006.00812.x.
Fildani, A., Hubbard, S.M., Covault, J.A., Maier, K.L., Romans, B.W., Traer, M., and Rowland, J.C., 2013, Erosion at inception of deep-sea channels: Marine and Petroleum Geology, v. 41, p. 48–61, doi:10.1016/j.marpetgeo.2012.03.006.
Flood, R.D., et al., 1995, Proceedings of the Ocean Drilling Program: Initial reports, Volume 155: College Station, TX (Ocean Drilling Program), 702 p., doi:10.2973/odp.proc.ir.155.1995.
Fosdick, J.C., Romans, B.W., Fildani, A., Bernhardt, A., Calderon, M., and Graham, S.A., 2011, Kinematic history of the Cretaceous–Neogene Patagonian fold-thrust belt and Magallanes foreland basin, Chile and Argentina (51 30′S): Geological Society of America Bulletin, v. 123, p. 1679–1698, doi:10.1130/B30242.1.
Funk, J.E., Slatt, R.M., and Pyles, D.R., 2012, Quantification of static connectivity between deep-water channels and stratigraphically adjacent architectural elements using outcrop analogs: American Association of Petroleum Geologists Bulletin, v. 96, p. 277–300, doi:10.1306/07121110186.
Garcia, M., and Parker, G., 1989, Experiments on hydraulic jumps in turbidity currents near a canyon-fan transition: Science, v. 245, p. 393–396, doi:10.1126/science.245.4916.393.
Gardner, M.H., and Borer, J.M., 2000, Submarine channel architecture along a slope to basin profile, Brushy Canyon Formation, west Texas, *in* Bouma, A.H., and Stone, C.G., eds., Fine-grained turbidite systems: Society for Sedimentary Geology (SEPM) Special Publication 68, p. 195–211.
Gardner, M.H., Borer, J.M., Melick, J.J., Mavilla, N., Dechesne, M., and Wagerle, R.M., 2003, Stratigraphic process-response model for submarine channels and related features from studies of Permian Brushy Canyon outcrops, west Texas: Marine and Petroleum Geology, v. 20, p. 757–787, doi:10.1016/j.marpetgeo.2003.07.004.
Gee, M.J.R., and Gawthorpe, R.L., 2007, Early evolution of submarine channels offshore Angola revealed by three-dimensional seismic data, *in* Davies, R.J., et al., eds., Seismic geomorphology: Applications to hydrocarbon exploration and development: Geological Society, London, Special Publication 277, p. 223–235, doi:10.1144/GSL.SP.2007.277.01.13.
Gee, M.J.R., Gawthorpe, R.L., Bakke, K., and Friedmann, S.J., 2007, Seismic geomorphology and evolution of submarine channels from the Angolan continental margin: Journal of Sedimentary Research, v. 77, p. 433–446, doi:10.2110/jsr.2007.042.
Hodgson, D.M., Di Celma, C., Brunt, R.L., and Flint, S.S., 2011, Submarine slope degradation and aggradation and the stratigraphic evolution of channel-levee systems: Journal of the Geological Society [London], v. 168, p. 625–628, doi:10.1144/0016-76492010-177.
Hofstra, M., Hodgson, D.M., Peakall, J., and Flint, S.S., 2015, Giant scour-fills in ancient channel-lobe transition zones: Formative processes and depositional architecture: Sedimentary Geology, v. 329, p. 98–114, doi:10.1016/j.sedgeo.2015.09.004.
Hubbard, S.M., and Shultz, M.R., 2008, Deep burrows in submarine fan-channel deposits of the Cerro Toro Formation (Cretaceous), Chilean Patagonia: Implications for firmground development and colonization in the deep sea: Palaios, v. 23, p. 223–232, doi:10.2110/palo.2006.p06-127r.
Hubbard, S.M., Fildani, A., Romans, B.W., Covault, J.A., and McHargue, T.R., 2010, High-relief slope clinoform development: Insights from outcrop, Magallanes Basin, Chile: Journal of Sedimentary Research, v. 80, p. 357–375, doi:10.2110/jsr.2010.042.
Hubbard, S.M., Covault, J.A., Fildani, A., and Romans, B.W., 2014, Sediment transfer and deposition in slope channels: Deciphering the record of enigmatic deep-sea processes from outcrop: Geological Society of America Bulletin, v. 126, p. 857–871, doi:10.1130/B30996.1.
Hughes Clarke, J.E., Vidiera Marques, C.R., and Pratomo, D., 2013, Imaging active mass-wasting and sediment flows on a fjord delta, Squamish, British Columbia, *in* Krastel, S., et al., eds., Submarine mass movements and their consequences: Advances in Natural and Technological Hazards Research 37: Cham, Switzerland, Springer International Publishing, p. 249–260, doi:10.1007/978-3-319-00972-8_22.
Ito, M., Ishikawa, K., and Nishida, N., 2014, Distinctive erosional and depositional structures formed at a canyon mouth: A lower Pleistocene deep-water succession in the Kazusa forearc basin on the Boso Peninsula, Japan: Sedimentology, v. 61, p. 2042–2062, doi:10.1111/sed.12128.
Jegou, I., Savoye, B., Pirmez, C., and Droz, L., 2008, Channel-mouth lobe complex of the recent Amazon Fan: The missing piece: Marine Geology, v. 252, p. 62–77, doi:10.1016/j.margeo.2008.03.004.
Jobe, Z.R., Sylvester, Z., Parker, A.O., Howes, N., Slowey, N., and Pirmez, C., 2015, Rapid adjustment of submarine channel architecture to changes in sediment supply: Journal of Sedimentary Research, v. 85, p. 729–753, doi:10.2110/jsr.2015.30.
Kane, I.A., and Hodgson, D.M., 2011, Sedimentological criteria to differentiate submarine channel levee subenvironments: Exhumed examples from the Rosario Fm. (Upper Cretaceous) of Baja California, Mexico, and the Fort Brown Fm. (Permian), Karoo Basin, S. Africa: Marine and Petroleum Geology, v. 28, p. 807–823, doi:10.1016/j.marpetgeo.2010.05.009.
Kenyon, N.H., and Millington, J., 1995, Contrasting deep-sea depositional systems in the Bering Sea, *in* Pickering, K.T., et al., eds., Atlas of deep water environments: Architectural style in turbidite systems: London, Chapman and Hall, p. 196–202.
Kostic, S., 2011, Modeling of submarine cyclic steps: Controls on their formation, migration and architecture: Geosphere, v. 7, p. 294–304, doi:10.1130/GES00601.1.
Kostic, S., 2014, Upper flow regime bedforms on levees and continental slopes: Turbidity current flow dynamics in response to fine-grained sediment waves: Geosphere, v. 10, p. 1094–1103, doi: 1130/GES01015.1.
Kostic, S., and Parker, G., 2006, The response of turbidity currents to a canyon-fan transition: Internal hydraulic jumps and depositional signatures: Journal of Hydraulic Research, v. 44, p. 631–653, doi:10.1080/00221686.2006.9521713.
Lien, T., Walker, R.G., and Martinsen, O.J., 2003, Turbidites in the Upper Carboniferous Ross Formation, western Ireland: Reconstruction of a channel and spillover system: Sedimentology, v. 50, p. 113–148, doi:10.1046/j.1365-3091.2003.00541.x.
Lowe, D.R., 1982, Sediment gravity flows: II. Depositional models with special reference to the deposits of high-density turbidity currents: Journal of Sedimentary Petrology, v. 52, p. 279–297, doi:10.1306/212F7F31-2B24-11D7-8648000102C1865D.
Macauley, R.V., and Hubbard, S.M., 2013, Slope channel sedimentary processes and stratigraphic stacking, Cretaceous Tres Pasos Formation slope system, Chilean Patagonia: Marine and Petroleum Geology, v. 41, p. 146–162, doi:10.1016/j.marpetgeo.2012.02.004.

Macdonald, H.A., 2010, Flutes, megaflutes and erosional bedforms: A reappraisal of their dynamics [Ph.D. thesis]: Leeds, UK, University of Leeds, 275 p.

Macdonald, H.A., Wynn, R.B., Huvenne, V.A.I., Peakall, J., Masson, D.G., Weaver, P.P.E., and McPhail, S.D., 2011, New insights into the morphology, fill, and remarkable longevity (>0.2 m.y.) of modern deep-water erosional scours along the northeast Atlantic margin: Geosphere, v. 7, p. 845–867, doi:10.1130/GES00611.1.

Maier, K.L., Fildani, A., Paull, C.K., Graham, S.A., McHargue, T.R., Caress, D.W., and McGann, M., 2011, The elusive character of discontinuous deep-water channels: New insights from Lucia Chica channel system, offshore California: Geology, v. 39, p. 327–330, doi:10.1130/G31589.1.

Maier, K.L., Fildani, A., McHargue, T.R., Paull, C.K., Graham, S.A., and Caress, D.W., 2012, Punctuated deep-water channel migration: High-resolution subsurface data from the Lucia Chica channel system, offshore California, U.S.A.: Journal of Sedimentary Research, v. 82, p. 1–8, doi: 10.2110/jsr.2012.10.

Maier, K.L., Fildani, A., Paull, C.K., Graham, S.A., and Caress, D.W., 2013, Deep-sea channel evolution and stratigraphic architecture from inception to abandonment from high-resolution autonomous underwater vehicle surveys offshore central California: Sedimentology, v. 60, p. 935–960, doi:10.1111/j.1365-3091.2012.01371.x.

Marini, M., Milli, S., Ravnås, R., and Moscatelli, M., 2015, A comparative study of confined v. semi-confined turbidite lobes from the Lower Messinian Laga Basin (Central Apennines, Italy): Implications for assessment of reservoir architecture: Marine and Petroleum Geology, v. 63, p. 142–165, doi:10.1016/j.marpetgeo.2015.02.015.

Mayall, M., Jones, E., and Casey, M., 2006, Turbidite channel reservoirs: Key elements in facies prediction and effective development: Marine and Petroleum Geology, v. 23, p. 821–841, doi:10.1016/j.marpetgeo.2006.08.001.

McHargue, T.R., Pyrcz, M.J., Sullivan, M.D., Clark, J.D., Fildani, A., Romans, B.W., Covault, J.A., Levy, M., Posamentier, H.W., and Drinkwater, N.J., 2011, Architecture of turbidite channel systems on the continental slope: Patterns and predictions: Marine and Petroleum Geology, v. 28, p. 728–743, doi:10.1016/j.marpetgeo.2010.07.008.

Middleton, G.V., 1965, Antidune cross-bedding in a large flume: Journal of Sedimentary Petrology, v. 35, p. 922–927, doi:10.1306/74D713AC-2B21-11D7-8648000102C1865D.

Moody, J.D., Pyles, D.R., Clark, J.D., and Bouroullec, R., 2012, Quantitative outcrop characterization of an analog to weakly confined submarine channel systems: Morillo 1 member, Ainsa Basin, Spain: American Association of Petroleum Geologists Bulletin, v. 96, p. 1813–1841, doi:10.1306/01061211072.

Morris, E.A., Hodgson, D.M., Flint, S.S., Brunt, R.L., Butterworth, P.J., and Verhaeghe, J., 2014, Sedimentology, stratigraphic architecture, and depositional context of submarine frontal-lobe complexes: Journal of Sedimentary Research, v. 84, p. 763–780, doi:10.2110/jsr.2014.61.

Morris, S.A., Kenyon, N.H., Limonov, A.H., and Alexander, J., 1998, Downstream changes of large-scale bedforms in turbidites around the Valencia channel mouth, north-west Mediterranean: Implications for palaeoflow reconstruction: Sedimentology, v. 45, p. 365–377, doi:10.1046/j.1365-3091.1998.0160f.x.

Mutti, E., and Normark, W.R., 1987, Comparing examples of modern and ancient turbidite systems: Problems and concepts, *in* Leggett, J.K., and Zuffa, G.G., eds., Marine clastic sedimentology: Concepts and case studies: London, Graham and Trotman, p. 1–38.

Mutti, E., and Normark, W.R., 1991, An integrated approach to the study of turbidite systems, *in* Weimer, P., and Link, M.H., eds., Seismic facies and sedimentary processes of submarine fans and turbidite systems: New York, Springer Verlag, p. 75–106.

Mutti, E., Remacha, E., Sgavetti, M., Rosell, J., Valloni, R., and Zamorano, M., 1985, Stratigraphy and facies characteristics of the Eocene Hecho Group turbidite systems, south-central Pyrenees, *in* Mila, M.D., and Rosell, J., eds., Excursion guidebook of the 6th European regional meeting of the International Association of Sedimentologists: Lleida, Spain, Institut d'Estudis Ilerdencs, Diputació Provincial de Lleida, p. 521–576.

Normark, W.R., 1970, Growth patterns of deep-sea fans: American Association of Petroleum Geologists Bulletin, v. 54, p. 2170–2195.

Normark, W.R., and Piper, D.J., 1983, Navy Fan, California Borderland: Growth patterns and depositional processes: Geo-Marine Letters, v. 3, p. 101–108, doi:10.1007/BF02462454.

Normark, W.R., and Piper, D.J.W., 1991, Initiation processes and flow evolution of turbidity currents: Implications for the depositional record, *in* Osborne, R.H., ed., From shoreline to abyss: Contributions to marine geology in honor of Francis Parker Shepard: SEPM (Society for Sedimentary Geology) Special Publication 46, p. 207–230, doi:10.2110/pec.91.09.0207.

Normark, W.R., Piper, D.J.W., and Hess, G.R., 1979, Distributary channels, sand lobes, and mesotopography of Navy submarine fan, California Borderland, with applications to ancient fan sediments: Sedimentology, v. 26, p. 749–774, doi:10.1111/j.1365-3091.1979.tb00971.x.

Normark, W.R., Paull, C.K., Caress, D.W., Ussler, W., and Sliter, R., 2009, Fine-scale relief related to late Holocene channel shifting within the floor of the upper Redondo Fan, offshore southern California: Sedimentology, v. 56, p. 1690–1704, doi:10.1111/j.1365-3091.2009.01052.x.

Palanques, A., Kenyon, N.H., Alonso, B., and Limonov, A., 1995, Erosional and depositional patterns in the Valencia Channel mouth: An example of a modern channel-lobe transition zone: Marine and Geophysical Researches, v. 17, p. 503–517, doi: 10.1007/BF01204341.

Parker, G., 1996, Some speculations on the relation between channel morphology and channel-scale flow structures, *in* Ashworth, P.J., et al., eds., Coherent flow structures in open channels: New York, John Wiley and Sons, p. 423–458.

Paull, C.K., Ussler, W., Caress, D.W., Lundsten, E., Covault, J.A., Maier, K.L., Xu, J., and Augenstein, S., 2010, Origins of large crescent-shaped bedforms within the axial channel of Monterey Canyon, offshore California: Geosphere, v. 6, p. 755–774, doi:10.1130/GES00527.1.

Paull, C.K., Caress, D.W., Ussler, W., Lundsten, E., and Meiner-Johnson, M., 2011, High-resolution bathymetry of the axial channels within Monterey and Soquel submarine canyons, offshore central California: Geosphere, v. 7, p. 1077–1101, doi:10.1130/GES00636.1.

Pickering, K.T., Hodgson, D.M., Platzman, E., Clark, J.D., and Stephens, C., 2001, A new type of bedform produced by backfilling processes in a submarine channel, late Miocene, Tabernas-Sorbas Basin, SE Spain: Journal of Sedimentary Research, v. 71, p. 692–704, doi:10.1306/2DC40960-0E47-11D7-8643000102C1865D.

Piper, D.J.W., and Normark, W.R., 1983, Turbidite depositional patterns and flow characteristics, Navy Submarine Fan, California Borderland: Sedimentology, v. 30, p. 681–694, doi:10.1111/j.1365-3091.1983.tb00702.x.

Pirmez, C., Beaubouef, R.T., Friedman, S.J., and Mohrig, D.C., 2000, Equilibrium profile and base level in submarine channels: Examples from late Pleistocene systems and implications for the architecture of deepwater reservoirs, *in* Weimer, P., et al., eds., Deep-water reservoirs of the world: Gulf Coast Section SEPM 20th Annual Research Conference, p. 782–805, doi:10.5724/gcs.00.15.0782.

Posamentier, H.W., 2003, Depositional elements associated with a basin floor channel levee system: Case study from the Gulf of Mexico: Marine and Petroleum Geology, v. 20, p. 677–690, doi:10.1016/j.marpetgeo.2003.01.002.

Posamentier, H.W., and Kolla, V., 2003, Seismic geomorphology and stratigraphy of depositional elements in deep-water settings: Journal of Sedimentary Research, v. 73, p. 367–388, doi:10.1306/111302730367.

Postma, G., and Cartigny, M.J.B., 2014, Supercritical and subcritical turbidity currents and their deposits—A synthesis: Geology, v. 42, p. 987–990, doi:10.1130/G35957.1.

Postma, G., Cartigny, M.J.B., and Kleverlaan, K., 2009, Structureless, coarse-tail graded Bouma Ta formed by internal hydraulic jump of the turbidity current?: Sedimentary Geology, v. 219, p. 1–6, doi:10.1016/j.sedgeo.2009.05.018.

Postma, G., Kleverlaan, K., and Cartigny, M.J.B., 2014, Recognition of cyclic steps in sandy and gravelly turbidite sequences, and consequences for the Bouma facies model: Sedimentology, v. 61, p. 2268–2290, doi:10.1111/sed.12135.

Prather, B.E., 2003, Controls on reservoir distribution, architecture and stratigraphic trapping in slope settings: Marine and Petroleum Geology, v. 20, p. 529–545, doi:10.1016/j.marpetgeo.2003.03.009.

Prather, B.E., Booth, J.R., Steffens, G.S., and Craig, P.A., 1998, Classification, lithologic calibration, and stratigraphic succession of seismic facies of intraslope basins, deep-water Gulf of Mexico: American Association of Petroleum Geologists Bulletin, v. 82, p. 701–728.

Prélat, A., Hodgson, D.M., and Flint, S.S., 2009, Evolution, architecture and hierarchy of distributary deep-water deposits: A high-resolution outcrop investigation from the Permian Karoo Basin, South Africa: Sedimentology, v. 56, p. 2132–2154, doi:10.1111/j.1365-3091.2009.01073.x.

Prélat, A., Covault, J.A., Hodgson, D.M., Fildani, A., and Flint, S.S., 2010, Intrinsic controls on the range of volumes, morphologies, and dimensions of submarine lobes: Sedimentary Geology, v. 232, p. 66–76, doi:10.1016/j.sedgeo.2010.09.010.

Pyles, D.R., Jennette, D.C., Tomasso, M., Beaubouef, R.T., and Rossen, C., 2010, Concepts learned from a 3d outcrop of a sinuous slope channel complex: Beacon channel complex, Brushy Canyon Formation, west Texas, U.S.A.: Journal of Sedimentary Research, v. 80, p. 67–96, doi:10.2110/jsr.2010.009.

Romans, B.W., Fildani, A., Graham, S.A., Hubbard, S.M., and Covault, J.A., 2010, Importance of predecessor basin history on the sedimentary fill of a retroarc foreland basin: Provenance analysis of the Cretaceous Magallanes Basin, Chile (50–52°): Basin Research, v. 22, p. 640–658, doi:10.1111/j.1365-2117.2009.00443.x.

Romans, B.W., Fildani, A., Hubbard, S.M., Covault, J.A., Fosdick, J.C., and Graham, S.A., 2011, Evolution of deep-water stratigraphic architecture, Magallanes Basin, Chile: Marine and Petroleum Geology, v. 28, p. 612–628, doi:10.1016/j.marpetgeo.2010.05.002.

Rowland, J.C., Hilley, G.E., and Fildani, A., 2010, A test of initiation of submarine leveed channels by deposition alone: Journal of Sedimentary Research, v. 80, p. 710–727, doi:10.2110/jsr.2010.067.

Shor, A.N., Piper, D.J.W., Hughes Clarke, J.E., and Mayer, L.A., 1990, Giant flute-like scour and other erosional features formed by the 1929 Grand Banks turbidity current: Sedimentology, v. 37, p. 631–645, doi:10.1111/j.1365-3091.1990.tb00626.x.

Shultz, M.R., and Hubbard, S.M., 2005, Sedimentology, stratigraphic architecture, and ichnology of gravity flow deposits partially ponded in a growth-fault-controlled slope minibasin, Tres Pasos Formation (Cretaceous), southern Chile: Journal of Sediemntary Research, v. 75, p. 440-453.

Stevenson, C.J., Talling, P.J., Wynn, R.B., Masson, D.G., Hunt, J.E., Frenz, M., Akhmetzhanhov, A.M., and Cronin, B.T., 2013, The flows that left no trace: Very large-volume turbidity currents that bypassed sediment through submarine channels without eroding the sea floor: Marine and Petroleum Geology, v. 41, p. 186–205, doi:10.1016/j.marpetgeo.2012.02.008.

Stevenson, C.J., Jackson, C.A.-L., Hodgson, D.M., Hubbard, S.M., and Eggenhuisen, J.T., 2015, Sediment bypass in deep-water systems: Journal of Sedimentary Research, v. 85, p. 1058–1081, doi:10.2110/jsr.2015.63.

Stright, L., Stewart, J., Campion, K., and Graham, S.A., 2014, Geologic and seismic modeling of a coarse-grained deep-water channel reservoir analog (Black's Beach, La Jolla, California): American Association of Petroleum Geologists Bulletin, v. 98, p. 695–728, doi:10.1306/09121312211.

Strong, N., and Paola, C., 2008, Valleys that never were: Time surfaces versus stratigraphic surfaces: Journal of Sedimentary Research, v. 78, p. 579–593, doi:10.2110/jsr.2008.059.

Sullivan, M.D., Jensen, G.N., Goulding, F.J., Jennette, D.C., Foreman, J.L., and Stern, D., 2000, Architectural analysis of deep-water outcrops: Implications for exploration and development of the Diana sub-basin, western Gulf of Mexico, *in* Weimer, P., et al., eds., Global deep-water reservoirs: Gulf Coast Section SEPM (Society for Sedimentary Geology) Foundation 20th Annual Research Conference, p. 1010–1032, doi:10.5724/gcs.00.15.1010.

Sylvester, Z., Pirmez, C., and Cantelli, A., 2011, A model of submarine channel-levee evolution based on channel trajectories: Implications for stratigraphic architecture: Marine and Petroleum Geology, v. 28, p. 716–727, doi:10.1016/j.marpetgeo.2010.05.012.

Talling, P.J., Masson, D.G., Sumner, E.J., and Malgesini, G., 2012, Subaqueous sediment density flows: Depositional processes and deposit types: Sedimentology, v. 59, p. 1937–2003, doi:10.1111/j.1365-3091.2012.01353.x.

Van der Merwe, W.C., Hodgson, D.M., Brunt, R.L., and Flint, S.S., 2014, Depositional architecture of sand attached and sand-detached channel-lobe transition zones on an exhumed stepped slope mapped over a 2500 km^2 area: Geosphere, v. 10, p. 958–968, doi:10.1130/GES01035.1.

Vicente Bravo, J.C., and Robles, S., 1995, Large-scale mesotopographic bedforms from the Albian Black Flysch, northern Spain: Characterization, setting and comparison with recent analogous, *in* Pickering, K.T., et al., eds., Atlas of deep water environments: Architectural style in turbidite systems: London, Chapman and Hall, p. 216–226.

Wynn, R.B., Kenyon, N.H., Masson, D.G., Stow, D.A.V., and Weaver, P.E., 2002, Characterization and recognition of deep-water channel-lobe transition zones: American Association of Petroleum Geologists Bulletin, v. 86, p. 1441–1462, doi:10.1306/61EEDCC4-173E-11D7-8645000102C1865D.